Journal of Experimental Marine Biology and Ecology 585 (2025) 152092

Contents lists available at ScienceDirect

Journal of Experimental Marine Biology and Ecology

journal homepage: www.elsevier.com/locate/jembe

Sponge species from New Zealand may transform and degrade dissolved organic matter

Tanja Stratmann [a,b,c,*], Mario L.M. Miranda [d,e], Anna de Kluijver [c], Kathrin Busch [f], Michelle Kelly [g], Sadie Mills [h], Peter J. Schupp [i,j]

[a] Department of Estuarine & Delta Systems, NIOZ – Royal Netherlands Institute for Sea Research, Korringaweg 7, 4401 NT Yerseke, The Netherlands
[b] Department of Ocean Systems, NIOZ – Royal Netherlands Institute for Sea Research, Landsdiep 4, 1797 SZ 't Horntje (Texel), The Netherlands
[c] Department of Earth Sciences, Faculty of Geosciences, Utrecht University, Vening Meineszgebouw A, Princetonlaan 8a, 3584 CB Utrecht, The Netherlands
[d] Universidad de Panamá, Vicerrectoría de Investigación y Posgrado, Laboratorio de la Calidad del Agua y Aire, P.O. Box 0824, Panama City, Panama
[e] Sistema Nacional de Investigación, Secretaría Nacional de Ciencia y Tecnologías (SNI-SENACYT), P.O. Box 0816-02852, Panama City, Panama
[f] Division of Marine Ecology, Marine Symbioses, GEOMAR Helmholtz-Centre for Ocean Research, Düsternbrooker Weg 20, 24105 Kiel, Germany
[g] National Centre for Coasts and Oceans, National Institute of Water and Atmospheric Research, 41 Market Place Viaduct Harbour, 1010 Auckland, New Zealand
[h] NIWA Invertebrate Collection, National Institute of Water and Atmospheric Research, 301 Evans Bay Parade, Hataitai, Wellington 6021, New Zealand
[i] Helmholtz Institute for Functional Marine Biodiversity, University of Oldenburg, Ammerländer Heerstraße 231, 26129 Oldenburg, Germany
[j] Institute for Chemistry and Biology of the Marine Environment, Carl von Ossietzky University of Oldenburg, Schleusenstraße 1, 26382 Wilhelmshaven, Germany

ARTICLE INFO

Keywords:
Parallel factor analysis (PARAFAC)
Emission-excitation matrix (EEM)
Long-chain fatty acids
PUFA

ABSTRACT

Sponges are an important component of shallow- and deep-water ecosystems enhancing eukaryotic biodiversity via diverse endo- and epibiota and by providing three dimensional habitats for benthic invertebrates and fishes. Sponge biodiversity is particularly high in the waters around New Zealand (Southwest Pacific), where we collected two shallow- and two deep-water sponge species (*Tedania* sp., *Suberea meandrina*, *Farrea raoulensis*, *Artemisina* sp.) for *ex-situ* incubation experiments to measure processing of dissolved organic matter (DOM). Several sponge species take up DOM and make it available to other fauna as detritus or as sponge biomass, a process known as sponge loop. However, it is unknown whether the selected sponge species are able to consume dissolved organic carbon (DOC) and/or total dissolved nitrogen (TDN).

We measured DOC and TDN fluxes and linked it to the bacterial communities of the sponge holobiont to address research hypothesis 1. It stated that high-microbial abundance (HMA) sponges consume more DOM than low-microbial abundance (LMA) sponges. Changes in fluorescent dissolved organic matter (FDOM) over time were investigated to address research hypothesis 2. It proposed that the fluorescence intensity F_{max} of fluorophores decreased in incubations that showed a significant loss in DOM. We assessed the biochemical and phospholipid-derived fatty acids (PLFAs) composition of sponge tissue to address hypothesis 3. It suggested that the PLFLA composition of sponges differs between sponge classes. Finally, we tried to better understand the role of these sponges in nutrient cycling around New Zealand by combining data from all analyses.

Based on the community composition of the sponge-associated bacteria, we classified *Tedania* sp., *S. meandrina*, and *Artemisina* sp. as HMA sponges and *F. raoulensis* as LMA sponge. We did not measure a significant DOC flux and only the release of TDN by *Tedania* sp. was significantly different from 0 μmol TDN g org. C^{-1} d^{-1}. The presence of four fluorophores were detected in the FDOM pool: 2 tryptophan- and protein-like fluorophores (C1, C2), 1 humic-like fluorophore (C3), and 1 tyrosine-like fluorophore (C4). However, we could not validate hypothesis 2, because F_{max} of C1 decreased significantly in *S. meandrina* incubations, whereas F_{max} of C2 grew in the same incubations. F_{max} of C3 increased in *Tedania* sp. incubations, in which F_{max} of C4 decreased. In comparison, F_{max} of C4 in *S. meandrina* rose. The PLFA composition of sponge tissue was dominated by long-chain fatty acids, saturated fatty acids, and monosaturated fatty acids, and most PLFAs were sponge- and bacteria-specific. We could not confirmed hypothesis 3, either, because the PLFA composition of the

* Corresponding author at: Department of Estuarine & Delta Systems, NIOZ – Royal Netherlands Institute for Sea Research, Korringaweg 7, 4401 NT Yerseke, The Netherlands.
E-mail address: tanja.stratmann@nioz.nl (T. Stratmann).

https://doi.org/10.1016/j.jembe.2025.152092
Received 29 September 2024; Received in revised form 16 February 2025; Accepted 19 February 2025
Available online 28 February 2025

hexactinellid sponge included seven identified PLFAs, whereas the PLFA composition of the demosponges ranged from three to 29 identified PLFAs.

1. Introduction

Marine sponges (phylum Porifera) are mostly suspension-feeding, sessile metazoans (though see Hestetun et al., 2016; Morganti et al., 2021; Vacelet and Boury-Esnault, 1995) whose global distribution stretches from the Arctic (e.g., Morganti et al., 2022; Ramirez-Llodra et al., 2024; Rybakova et al., 2020) to the Southern Ocean (e.g., Downey et al., 2012; Kersken et al., 2014). They occur in all water depths from the intertidal zone (e.g., Barnes, 1999; Gastaldi et al., 2018) to deep-sea abyssal plains (e.g., Beaulieu, 2001; Kersken et al., 2019), and may contribute substantially to benthic density and biomass in sponge grounds (Cathalot et al., 2015; Hawkes et al., 2019; Maldonado et al., 2017; McIntyre et al., 2016; Morganti et al., 2022; Ramiro-Sánchez et al., 2019) and in tropical coral reefs (De Goeij et al., 2017; Diaz and Rützler, 2001). At the continental slope of Canada, sponges form large glass sponge reefs (Chu and Leys, 2010; Dunham et al., 2018) that are 9000 years old (Conway et al., 2001). Globally, the highest sponge biodiversities can be found in the northern Gulf of Mexico, the temperate Northern Atlantic including the Mediterranean Sea, the Central Indo-Pacific, and temperate Australasia (Spalding et al., 2007; Van Soest et al., 2012). Waters around New Zealand, in particular, host a minimum of 1361 different species (Kelly and Sim-Smith, 2023) and several new species have been described in recent years (e.g., Dohrmann et al., 2023; Reiswig et al., 2021).

Sponges are holobionts (Webster and Taylor, 2012) whose volume can consist to 38 % of microbial cells (Vacelet, 1975). Sponge species with particularly high densities of symbiotic microorganisms (10^8 to 10^{10} microorganisms g^{-1} sponge tissue; (Hentschel et al., 2006)) are known as high-microbial abundance (HMA) sponges, whereas sponges with symbiotic microbial densities comparable to densities of microorganisms in seawater are known as low-microbial abundance sponges (LMA) sponges (10^5 to 10^6 bacteria g^{-1} sponge tissue; Hentschel et al., 2006). LMA sponges often host a bacterial core community dominated by a single bacteria clade that differs among sponge specimens (Erwin et al., 2015; Giles et al., 2013). In comparison, HMA sponges host a bacterial community that is more diverse and clearly different from the bacterial community of LMA sponges (Erwin et al., 2015; Giles et al., 2013).

Suspension-feeding sponges filter bacterioplankton (de Goeij et al., 2008b; Scheffers et al., 2004; Yahel et al., 2006) and particulate organic matter (POM) (Hadas et al., 2009; McMurray et al., 2016) out of the water column with pumping rates (ml s^{-1} ml^{-1} sponge) of 0.03 (*Cinachyrella cavernosa* (Lamarck, 1815)) to 17.3 (*Aphrocallistes vastus* Schulze, 1886; Dahihande and Thakur, 2019; Leys et al., 2011) and filtration efficiencies of 23 % (*Rhopaloeides odorabile* Thompson, Murphy, Bergquist & Evans, 1987) to 99 % (*Sarcotragus spinosulus* Schmidt, 1862) for bacteria (Massaro et al., 2012; Trani et al., 2021). Sponges, such as *Cliona orientalis* Thiele, 1900, *Ircinia felix* (Duchassaing & Michelotti, 1864), or *Vazella pourtalesii* (Schmidt, 1870), also consume dissolved organic matter (DOM) (Achlatis et al., 2019; Archer et al., 2017; Bart et al., 2020) with DOM removal rates (μmol C g DW^{-1}_{sponge} h^{-1}) of 3.70 ± 0.26 (*Geodia barretti* Bowerbank, 1858) to 56.1 ± 19.9 (*Acantheurypon spinispinosum* (Topsent, 1904)) (Bart et al., 2020).

Several sponges (e.g., *Halisarca caerulea* Vacelet & Donadey, 1987, *Haliclona* (*Reniera*) *implexiformis* (Hechtel, 1965), *Chondrilla caribensis* Rützler, Duran & Piantoni, 2007, *Scopalina ruetzleri* (Wiedenmayer, 1977), *Mycale* (*Carmia*) *fistulifera* (Row, 1911), *Negombata magnifica* (Keller, 1889), *Hymedesmia* (*Stylopus*) *coriacea* (Fristedt, 1885), *G. barretti, Mycale (Mycale) lingua* (Bowerbank, 1866) (de Goeij et al., 2013; Maier et al., 2020; Rix et al., 2018, 2016)) convert this DOM and POM into particulate detritus that can be taken up by associated fauna as proposed in the so-called "detrital sponge loop" hypothesis (Bart et al., 2021a; de Goeij et al., 2013). Especially space-limited encrusting sponges can have high cell turnover rates (18–70 % turnover of choanocyte cells (Alexander et al., 2014)) and convert up to ~40 % (Rix et al., 2016) of the DOM they take up into detritus and fecal pellets. In comparison, in the "predatory sponge loop" (Bart et al., 2021a; McMurray et al., 2018; Pawlik and McMurray, 2020) carbon (C) is transferred through the food web when sponges with massive growth forms, like *Agelas tubulata* Lehnert & van Soest, 1996, *Ircinia strobilina* (Lamarck, 1816), or *Verongula gigantea* (Hyatt, 1875), assimilate DOM (Maier et al., 2020; McMurray et al., 2018), convert its C into biomass, and subsequently pass it on to predators when the sponges are predated upon by spongivores, such as starfish, sea turtles, fish, or nudibranchs (Belmonte et al., 2015; Dunlap and Pawlik, 1998; Meylan, 1988; Stratmann et al., 2022). In both versions of the sponge loop, sponges contribute to recycling of nutrients (particularly of C) and support the existence of biological hotspots in food-deprived ecosystems (de Goeij et al., 2013; Maier et al., 2020; Morganti et al., 2022; Stratmann et al., 2022). However, so far, it is unknown, whether sponges from New Zealand are involved in any of the two sponge loop versions and whether they are able to process DOM.

DOM is operationally defined as organic matter that passes through filters with pore sizes of 0.2 μm to 0.7 μm and includes fatty acids, vitamins, sugars, amino acids, proteins, lignins, and polysaccharides (Repeta, 2015). About 90 % of the DOM pool, however, is undescribed and consists of complex degradation products of unknown origin (Repeta, 2015). The C-containing fraction of DOM is called dissolved organic carbon (DOC) and the nitrogen (N)-containing fraction dissolved organic nitrogen (DON). DOC is the largest organic C pool in the oceans (662 Pg C; Hansell et al., 2009) and consists of labile, semi-labile and semi-refractory, and refractory DOC. Labile DOC has a turnover of minutes to days (Fuhrmann and Ferguson, 1986; Keil and Kirchman, 1999) and contributes only <0.2 Pg C (=0.03 % of global DOC pool) (Repeta, 2015). Semi-labile and semi-refractory DOC contribute 20 Pg C (= 3 % of global DOC pool) (Hansell et al., 2012) with a turnover of months to years (Hansell et al., 2012) and refractory DOC (including refractory and ultra-refractory DOC) is the largest pool with >642 Pg C (=97 % of global DOC pool) (Hansell et al., 2012) and a turnover of centuries to millennia (Bauer et al., 1992; Druffel et al., 2019). Parts of DOM is colored and referred to as colored dissolved organic matter (CDOM), which absorbs light of the visible and UV spectrum (Coble, 2007). A fraction of this CDOM in turn exhibits blue fluorescence and is referred to as fluorescent DOM (FDOM). It may serve as an "optical marker" (Stedmon and Nelson, 2015) for protein-like and humic-like fluorophores (Coble, 2007).

Fatty acids, building blocks of lipids, are more diverse in sponges than in other aquatic fauna (Rod'kina, 2005). Their specific composition varies among sponge classes and is more similar in Hexactinellida and Demospongiae than in Calcarea (Thiel et al., 2002a). Hexactinellida, like *Acanthascus* (*Staurocalyptus*) sp. Ijima, 1897 or *Acanthascus* sp. Schulze, 1886, contain high concentrations of $C30\Delta^{5,9,23}$, whereas Demospongiae (e.g., *Spirastrella* sp. Schmidt, 1868, *Astrosclera willeyana* Lister, 1900, *Phakellia ventilabrum* (Linnaeus, 1767)) have high concentrations of $C26{:}1\Delta^{5,9}$ (Thiel et al., 2002a). In comparison, unsaturated long-chain fatty acids (LCFA, ≥C24) are absent in Calcarea sponges, such as *Sycon* sp. Risso, 1827 or *Leucetta* sp. Haeckel, 1872 (Thiel et al., 2002b). Sponges produce these LCFA via elongation of fatty acids with shorter chain length that originate from their diets (Carballeira et al., 1986; de Kluijver et al., 2021). Iso (*i*) and anteiso (*ai*)-branched fatty acids and mid-chain branched fatty acids (MBFAs), that are also found in sponges, however, are produced by their bacterial symbionts (Kaneda,

1991; Thiel et al., 1999). Hence, phospholipid-derived fatty acids (PLFAs) can be used to decipher which part of the sponge holobiont (i.e., the sponge or its microbiome) actively processes a food source, particularly when combined with stable isotope probing experiments with ^{13}C and/or ^{2}H. For instance, (Campana et al., 2021b) compared the uptake of three different ^{13}C-enriched DOM sources by tropical, shallow-water sponges. The authors detected ^{13}C incorporation into sponge-specific and bacteria-specific PLFAs, whereupon the total PLFA incorporation rate was the same for HMA and LMA sponges. However, HMA sponges incorporated more DOM into bacteria-specific PLFAs than LMA sponges (Campana et al., 2021b). In another study, (Stratmann et al., 2024b) assessed the uptake of ^{13}C-enriched bacterioplankton by sponges and detected ^{13}C incorporation into bacteria-specific, sponge-specific, and other PLFAs.

In this study, we measured *ex-situ* DOC and total dissolved nitrogen (TDN) fluxes in shallow-water (6 m water depth) and deep-water sponges (828 to 1448 m water depth) around New Zealand (Southwest Pacific). We tried to decipher FDOM components that were present in the incubations and assessed any differences in fatty acid and bacterial composition among the various sponge species. Based on these individual analyses, we addressed the following research hypotheses: 1) HMA sponges consumed more DOC and/or TDN than LMA sponges, 2) F_{max} of fluorophores decreased in incubations with a significant reduction in DOC/ TDN concentrations, and 3) the PLFA composition of sponges differs between Hexactinellida and Demospongiae.

2. Materials and methods

2.1. Sampling

Shallow-water sponges were collected by snorkeling at 6 m water depth at Denham Bay (Raoul Island, New Zealand; Fig. 1, Table 1). All sponges were transported in plastic bags filled with ambient seawater to R/V *Sonne* that stayed outside the 1 km exclusion zone around the Kermadec Islands. Deep-water sponges were collected randomly at water depths between 828 m and 1448 m (Fig. 1, Table 1) with the remotely operated vehicle (ROV) Kiel 6000 (Geomar, Germany) during R/V *Sonne* cruise SO254 (Simon, 2017) and transported in bioboxes filled with ambient seawater to R/V *Sonne*.

2.2. Ex-situ incubation experiments

For the *ex-situ* incubation experiments aboard R/V *Sonne*, sponges of the same putative species were incubated individually in three acid-washed (10 % HCl) closed incubation chambers (water volume: 1.26 L) that were equipped with magnetic stirrers (for chamber design see Fig. S1 in de Goeij et al. (2013)). A forth acid-washed incubation chamber of the same size filled with seawater served as control. Incubations with shallow-water sponges (*Tedania* sp. indet. ($n = 3$), *Suberea meandrina* (Kelly, 2015) ($n = 3$); Fig. 2) were conducted as light-incubations in a water bath in a temperature-controlled room (incubation temperature: 23.6 ± 1 °C), whereas incubations of deep-water sponges (*Farrea raoulensis* (Reiswig & Kelly, 2011) ($n = 3$), *Artemisina* sp. indet. ($n = 6$ specimens in 1 core); Fig. 2) were conducted in the dark in the fridge (incubation temperature: 5 °C).

Due to logistic constrained aboard the research vessel, sponges could not acclimatize for days to weeks in large tanks on board. Instead, the incubations were prepared immediately upon sponge retrieval: When sponges arrived aboard, either from the snorkeling trip (shallow-water species) or from the ROV dive (deep-water species), only those specimens were selected for the incubations that seemed healthy with wide open oscula which was interpreted as a sign of active pumping. Continuous active pumping was confirmed visually several times during the incubations.

Sponge specimens were transferred to the incubation chambers together with the ambient seawater in which they arrived at the vessel.

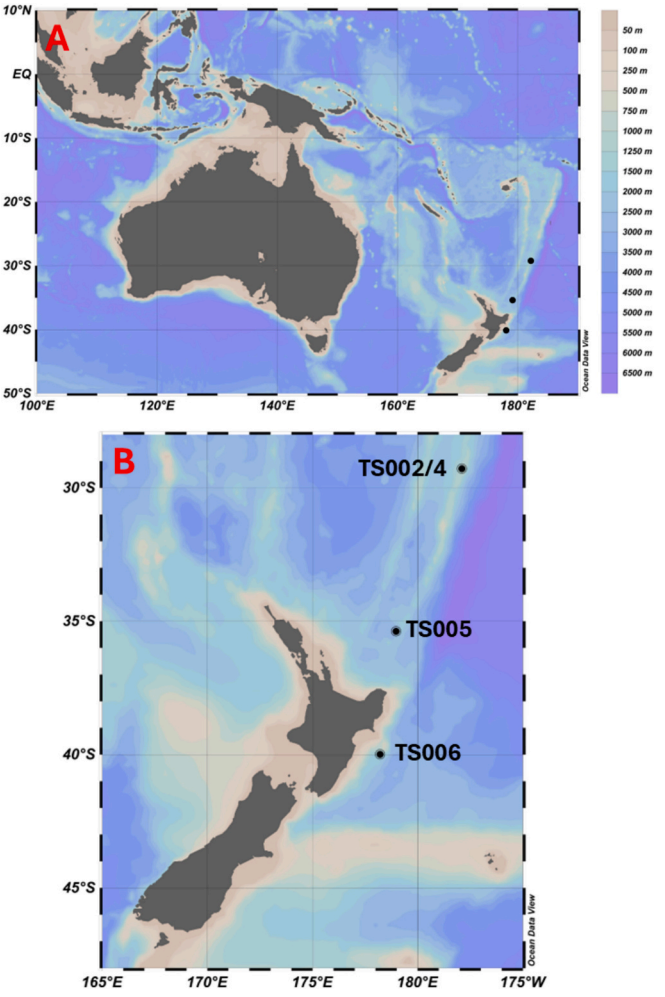

Fig. 1. Map of (A) the southwestern Pacific and Oceania (including Australia and New Zeeland) with (B) sampling sites (black dots) around New Zealand where shallow-water and deep-water sponges were collected for the incubations. Detailed information about species names and sampling depths are given in Table 1.

Whenever the chambers were not completely filled with the ambient water, additional shallow seawater was added to fill the chambers completely. A list with DOC and TDN concentrations at the beginning of the *ex-situ* incubations is shown in Table S1.

Every hour for five hours (before the start of the incubation: T0, after 1 h: T1, after 2 h: T2, etc.) triplicate water samples for DOC and TDN were taken with acid-rinsed syringes, filtered through GHP membrane syringe filters (0.2 µm pore size) into acid-washed 30 ml HDPE bottles, acidified to pH 2 with 25 % HCl and stored at 4 °C until analysis at the University of Oldenburg (Germany). Water samples for CDOM and FDOM analyses were taken at the same time intervals, filtered through the GHP membrane syringe filters (0.2 µm pore size) into acid-washed, pre-combusted 100 ml amber glass bottles and stored for 1 to 3 d at 4 °C until the samples were measured aboard R/V *Sonne*. These are standard procedure to take samples for DOC and TDN measurements in seawater and recommended in (Halewood et al., 2022). We only deviated from the recommendations in the choice of the pore size of the filters, as we selected 0.2 µm filters to exclude bacteria (Repeta, 2015). Filters with this pore size had been used in comparable sponge incubation studies in which DOC removal by sponges was measured (e.g., de Goeij et al., 2008b).

At the end of the incubations, dimensions (i.e., length *L*, width *W*, and height *H*) of each sponge specimen were measured to the nearest

Table 1
Detailed information about sampling location and species name of all collected sponges.

Sample ID	Geographical location	Latitude (°N)	Longitude (°E)	Depth (m)	T (°C)	Species [Class, Family]
TS002	Denham Bay, Raoul Island	-29.283	-177.900	6	25.0	*Tedania* sp. indet. [Demospongiae, Tedaniidae]
TS004	Denham Bay, Raoul Island	-29.283	-177.900	6	25.0	*Suberea meandrina* (Kelly, 2015) [Demospongiae, Aplysinellidae]
TS005	Southern Kermadec Ridge (Sponge Ridge)	-35.378	178.974	1448	6.0	*Farrea raoulensis* (Reiswig & Kelly, 2011) [Hexactinellida, Farreidae]
TS006	Seamount No. 986, off Hawkes Bay Shelf	-39.991	178.215	828	6.0	*Artemisina* sp. indet. [Demospongiae, Microcionidae]

Abbreviation: T = water temperature.

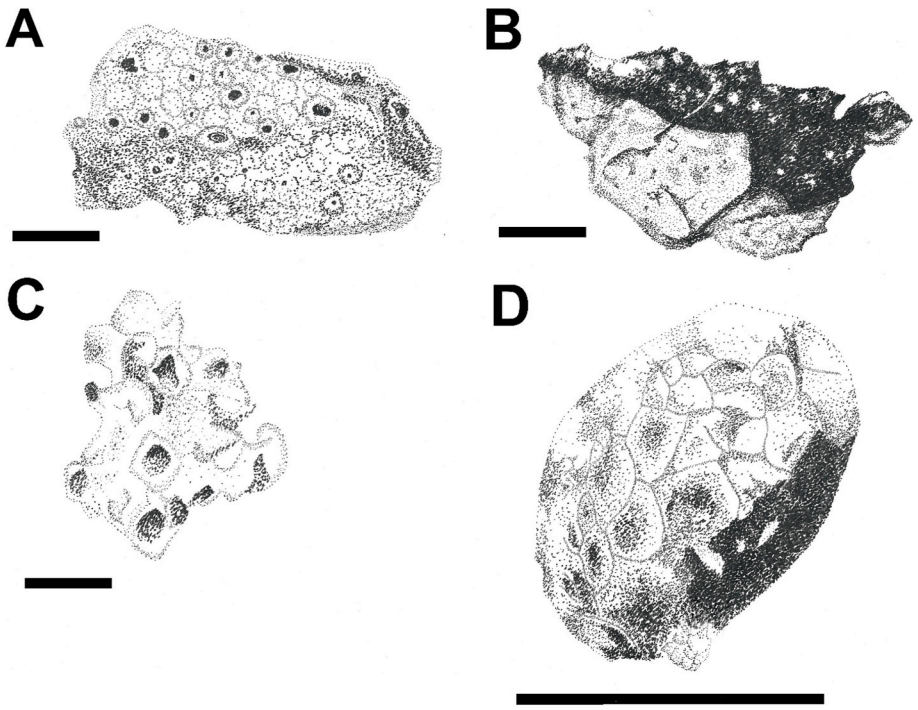

Fig. 2. Drawings of the four sponge species A) *Tedania* sp., B) *Suberea meandrina*, C) *Farrea raoulensis*, D) *Artemisina* sp. The black bar represents 1 cm. Illustrations by Tanja Stratmann.

millimeter. Subsamples for bacterial community analyses and species identification based on sponge spicules were taken with a scalpel from one sponge per incubation set (Table S1). Subsamples for bacterial community analysis were rinsed with sterilized seawater and stored at -80 °C after flash-freezing in liquid N, whereas subsamples for species identification were kept in ethanol (80 %).

The experimental design of the ex-situ experiments is presented in Fig. 3.

2.3. Sample processing

This is the second of a series of two papers describing N, oxygen, and C cycling in shallow-water and deep-water sponges around New Zealand. While this manuscript focused on DOM cycling, the paper by (Stratmann et al., 2024a) investigated inorganic nutrient cycling and oxygen consumption. As parts of the post-incubation sample processing (i.e., analyses of sponge tissue, fatty acids, and bacterial community composition of sponges) was identical in both papers, we decided to report the parts of the sample analyses that are identical in both papers only very briefly and instead refer the reader to the detailed description in (Stratmann et al., 2024a).

2.3.1. Analyses of sponge tissue

Sponge volume (V, cm^3) was determined by geometric shape (V_{GS}) using the eqs. 1 to 5 in (Stratmann et al., 2024a). Total wet mass (*WM*, g), total dry mass (*DM*, g), total ash-free dry mass (*AFDM*, g), and total org. C (%) were calculated using species-specific conversion factors (Table 2) developed for set of subsamples of sponge tissue, because not all sponge specimens reached the Netherlands intact due to post-incubation subsampling aboard.

Total carbon (*TC*, % DM)/ δ^{13}TC content and total nitrogen (*TN*, % DM)/ δ^{15}N content in freeze-dried, finely-ground, homogenized sponge tissue were determined at NIOZ-Yerseke (Yerseke, Netherlands) via an elemental analyzer coupled to an isotope ratio mass spectrometer (EA-c-IRMS) (for details see Stratmann et al. (2024a)). Samples for organic carbon (org. C, % DM)/ δ^{13}org. C content measurements were acidified with 20 µl 2 % HCl prior to EA-c-IRMS measurements.

2.3.2. Analysis of phospholipid-derived fatty acids

At Utrecht University (Utrecht, Netherlands) PLFAs from freeze-dried sponge tissue were extracted following a modified protocol of the Bligh and Dyer extraction method (Bligh and Dyer, 1959) which is published as protocol in (de Kluijver, 2021) and described in detail in (Stratmann et al., 2024a). After derivatizing the PLFAs into fatty acid methyl esters (FAMEs) via mild alkaline methylation as described in (de

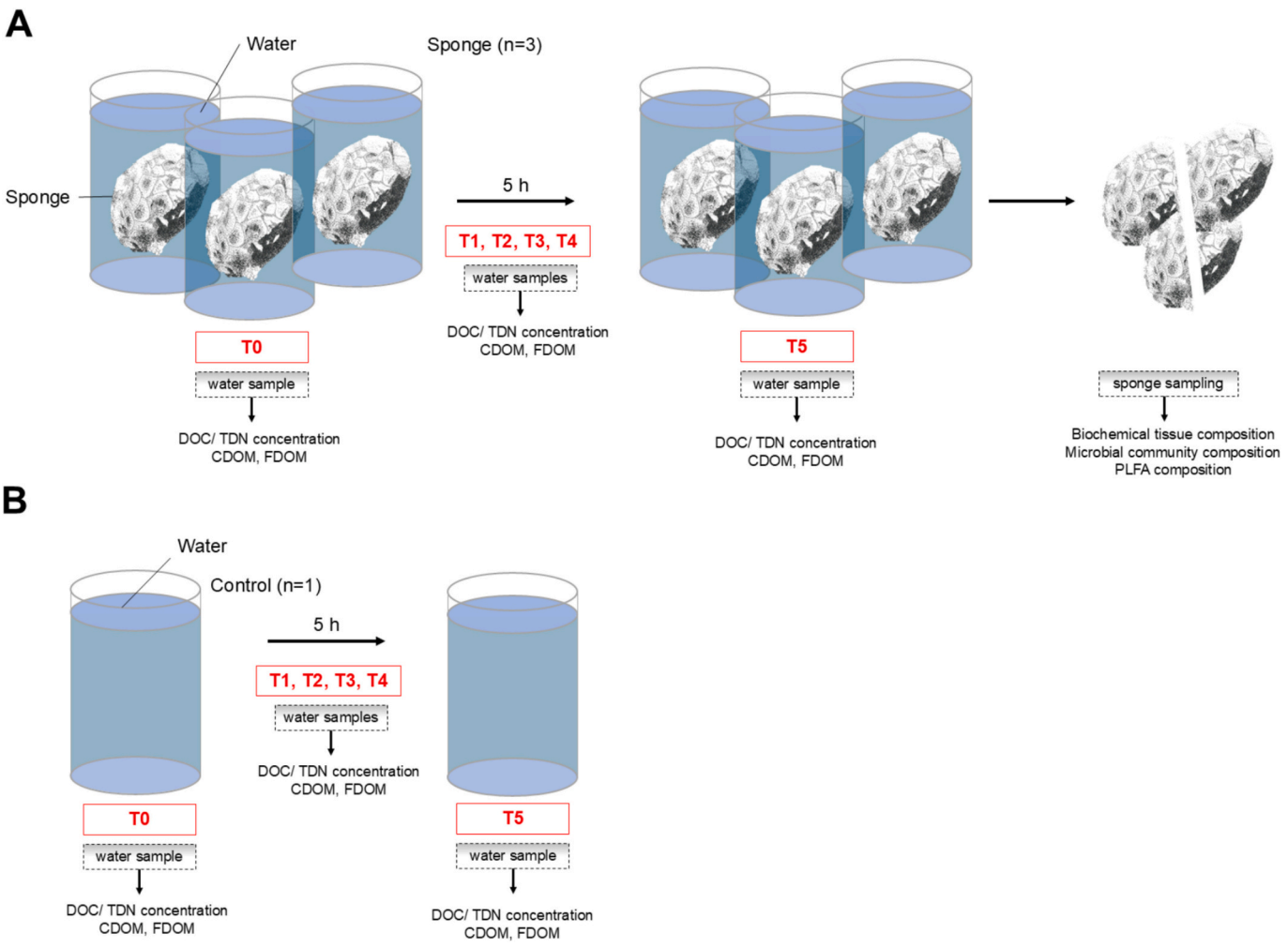

Fig. 3. Experimental design of the *ex-situ* experiment including (A) the sponge incubation and (B) the control incubation. Notice that "n" in the sponge incubations was always 3 except for sample ID TS006 where six small *Artemisina* sp. specimens were incubated together in one chamber.

Kluijver, 2021; Stratmann et al., 2024a), FAME concentrations were measured on a gas chromatograph with flame ionization detector (GC-FID) on a non-polar analytical column (CP-Sil5 CB; 25 m × 0.32 mm × 0.12 μm). Individual peaks in the chromatograms were identified by equivalent chain length (ECL) calculated based on known retention time of three standards ($C_{12:0}$-FAME, $C_{16:0}$-FAME, and $C_{19:0}$-FAME) and concentrations were calculated using the known concentration of $C_{19:0}$-FAME.

2.3.3. Analysis of sponge-associated bacterial community

At Geomar (Kiel, Germany) DNA of the subsamples for bacterial community analyses were extracted. DNA quantity and quality was confirmed by NanoDrop and gel electrophoresis after a PCR with the universal 16S rRNA gene primers. Bacterial V3 to V4 variable regions were amplified in a one-step PCR with primer pair 341F-806R (Caporaso et al., 2011; Muyzer et al., 1993). Samples were sequenced on a MiSeq platform (MiSeqFGx, Illumina) with v3 chemistry.

Amplicon sequences were processed within the QIIME2 platform (version 2019-10) (Bolyen et al., 2019) and amplicon sequence variants (ASVs) were generated from single-end reads with the DADA2 algorithm (Callahan et al., 2016). Representative ASVs were classified taxonomically using the SILVA database (version 138 99 % OTUs 16S) (Quast et al., 2013) with bacterial primer specific trained Naïve Bayes taxonomic classifiers.

2.3.4. Measurements of DOC, TDN

At the University of Oldenburg (Oldenburg, Germany) DOC and TDN concentrations were measured in triplicates by high temperature catalytic combustion with a Shimadzu TOC-VCPH/CPN total organic carbon analyzer coupled to a TNM-1 module. Deep Atlantic Seawater reference material (DSR, D. A. Hansell, University of Miami, USA) was measured during every run to evaluate instrument precision.

Table 2
Conversion factors (mean ± SE) for sponge volume (volume based on geometric shape, V_{GS}; volume determined via water displacement, V_{WD}) to sponge wet mass (*WM*), *WM* to dry mass (*DM*), *DM* to organic C (*org. C*), *DM* to total nitrogen (*TN*). "n" corresponds to the number of samples.

Sponge species	V_{GS}:V_{WD}	V_{WD}:*WM*	*WM*:*DM*	*DM*:*org. C*	*DM*:*TN*
Tedania sp. ($n = 3$)	0.58 ± 0.30	1.08 ± 0.11	$9.04 \times 10^{-2} \pm 1.38 \times 10^{-3}$	$8.22 \times 10^{-2} \pm 1.30 \times 10^{-2}$	$1.93 \times 10^{-2} \pm 1.86 \times 10^{-3}$
Suberea meandrina ($n = 3$)	$0.35 \pm 5.66 \times 10^{-2}$	1.09 ± 0.31	$0.22 \pm 7.02 \times 10^{-2}$	$4.84 \times 10^{-2} \pm 2.01 \times 10^{-2}$	$1.30 \times 10^{-2} \pm 5.56 \times 10^{-3}$
Farrea raoulensis ($n = 3$)	$0.17 \pm 9.40 \times 10^{-2}$	0.95 ± 0.43	$0.11 \pm 3.66 \times 10^{-2}$	$2.39 \times 10^{-2} \pm 1.03 \times 10^{-2}$	$4.88 \times 10^{-3} \pm 2.17 \times 10^{-3}$
Artemisina sp. ($n = 1$)	0.56	0.93	0.25	0.30	5.67×10^{-2}

2.3.5. Calculation of fluxes and initial net removal rates

Fluxes ($F_{i.DOC,\ TDN}$) of DOC and TDN (μmol g C^{-1} d^{-1}) were calculated as:

$$F_{i.DOC,TDN} = \frac{(LR_{slope,sponge} - LR_{slope,water}) \times (V_I - V_S)}{tC\ content_{sponge}}, \quad (1)$$

where $LR_{slope,sponge}$ and $LR_{slope,water}$ are the estimated slopes of the linear regression analyses done with the concentrations of DOC and TDN (μmol l^{-1}) collected over 5 h during the incubations as response (dependent) variable and time as predictor (independent) variable. $tC\ content_{sponge}$ corresponds to the org. C content of the incubated sponge (g C), V_I is the volume of the incubation chamber (= 1.26 l) and V_S is the sponge volume (l).

Initial net DOC and TDN removal rates were determined by applying a 2G-model following (de Goeij and van Duyl, 2007):

$$\frac{dDOC,TDN}{dt} = -(k_f C_f + k_s C_s), \quad (2)$$

where C_f was the fast removable DOC and TDN fraction, respectively, C_s was the slow removable DOC and TDN fraction, respectively, and k_f and k_s were the corresponding removal constants.

Eq. 2 was integrated to present DOC and TDN as a function of time (de Goeij and van Duyl, 2007):

$$DOC, TDN(t) = C_{f,0}e^{-k_f t} + C_{s,0}e^{-k_s t}. \quad (3)$$

The model variables of Eq. 3 were estimated by fitting a non-linear model with the Levenberg-Marquardt algorithm (Moré, 1978) (50 iterations) to the experimental data using the *nlsLM()* function from the *R* package 'minpack.lm' (version 1.2-4) (Elzhov et al., 2023) in *R* (version 4.3.0) (R-Core Team, 2022).

Whenever all the model variables could be estimated at a significance level of $\alpha = 0.05$, the initial DOC and TDN removal rates were calculated following (de Goeij and van Duyl, 2007) as:

$$Flux_{DOC,TDN} = -(k_f C_{f,0} + k_s C_{s,0}). \quad (4)$$

2.3.6. Measurement of FDOM and parallel factor analysis

During the expedition water samples were warmed to room temperature prior to spectrofluorometric measurements in a 1 cm quartz cuvette on an Aqualog spectrofluorometer (HORIBA Scientific, Japan) aboard R/V *Sonne*. Excitation/ emission matrix (EEM) scans were created for excitation wavelengths between 240 and 450 nm with 2 nm increments and for emission wavelengths between 240 and 450 nm with 0.5 nm increments. The excitation and emission bandwidths were 5 nm. EEMs of freshly-produced Milli-Q water served as blank.

EEMs were normalized to Raman Units (RU) after correcting for inner-filter effects (Lakowicz, 2006) and Raman and Rayleigh scatter (Senesi, 1990) using the *DrEEM* toolbox in Matlab version R2017a (MathWorks, Inc.) (Murphy et al., 2013). Subsequently, EEMs were decomposed into independent fluorescent components by parallel factor analysis (PARAFAC; Bro, 1998; Stedmon et al., 2003) using the *N-way* toolbox (Andersson and Bro, 2000) in Matlab as described by (Murphy et al., 2013). We constrained the PARAFAC model to non-negativity, initialized it randomly, and used a convergence criterion of 1.00×10^{-6}. One EEM sample was excluded as outlier ($n_{full\ dataset}$: 84, $n_{modelled\ samples}$: 83, $n_{excluded\ samples}$: 1). A four-component model could be validated through split-half analysis by splitting the dataset in four dataset halves that were combined six times and validated in three validation tests (AB vs. CD, AC vs. BD, AD vs. BC; $S_4C_6T_3$) (Murphy et al., 2013). This four-component model was able to explain 97.8 % of the sample variability.

Spectra of the identified fluorophores were compared with spectra of published FDOM components using the "OpenFluor" (https://openfluor.lablicate.com/) online spectral library for fluorescent, environmental organic compounds (Murphy et al., 2014). Published FDOM spectra were similar to spectra from this study when the Tucker congruence coefficient r_c (Lorenzo-Seva and ten Berge, 2006; Stedmon and Bro, 2008) was >0.95.

2.4. Statistical analysis

Statistical difference in the biochemical composition of tissue (i.e., TC, org. C, TN) between sponge species *Tedania* sp., *S. meandrina*, and *F. raoulensis* was assessed in *R* (R-Core Team, 2022) by 1-Way ANOVA ($\alpha = 0.05$) after homogeneity of variances was confirmed by the Bartlett test. The stable isotopic composition of the tissue (i.e., δ^{13}TC, δ^{13}org. C, δ^{15}N) between *Tedania* sp. and *S. meandrina* was tested again by 1-Way ANOVA after homogeneity of variances was confirmed by the Bartlett test.

For each species, a 1-sided Student's *t*-test ($\alpha = 0.05$) (for normally distributed data) or a 1-sample Wilcoxon test (for non-normal data) was used to test whether fluxes were significantly different from 0 μmol L^{-1} g C^{-1} d^{-1}.

A change in fluorescence intensity (R.U.) of the identified fluorescing components over time was tested for the three sponge incubations and the control incubation by robust regression analysis (Western, 1995) from the *MASS* package (Venables and Ripley, 2002) in *R*. A change in fluorophore intensity was considered significant for a specific sponge species and fluorophore, when the *F*-statistic ($\alpha = 0.05$) of the sponge incubation was significant, while the *F*-statistic ($\alpha = 0.05$) of the control incubation was not significant.

All data are presented as mean ± standard error (SE).

3. Results

3.1. Composition of sponge tissue

The investigated sponges from New Zealand had a water content of 85.3 ± 1.17 % ($n = 9$) and their dried tissue ($n = 8$) consisted of 18.3 ± 3.85 % TC, 17.5 ± 3.75 % org. C, and 4.34 ± 1.02 % TN. The lowest TC (3.65 ± 1.62 %), org. C (3.03 ± 1.22 %), and TN (0.62 ± 0.26 %) contents were measured in *F. raoulensis* ($n = 3$), whereas the sponge species with the highest TC (32.4 ± 1.33 %), org. C (31.1 ± 2.01 %), and TN (8.28 ± 0.42 %) contents was *S. meandrina* ($n = 3$). The δ^{13}org. C-value of the sponges ranged from -17.9 ‰ (*Artemisina* sp., $n = 1$) to -19.7 ± 0.10 ‰ (*F. raoulensis*, $n = 3$), the δ^{13}TC-value ranged from -18.4 ‰ (*Artemisina* sp., $n = 1$) to -20.3 ± 2.55 × 10^{-3}‰ (*F. raoulensis*, $n = 3$), and the δ^{15}N-value ranged from 5.39 ± 0.17 ‰ (*S. meandrina*, $n = 3$) to 20.9

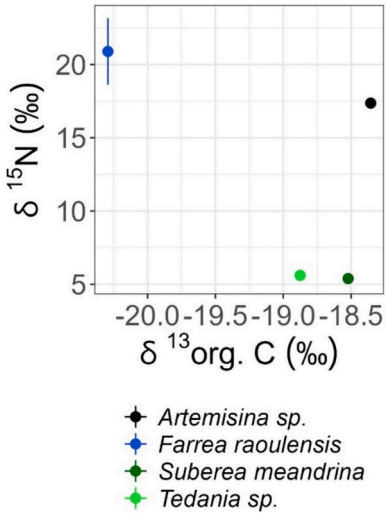

Fig. 4. Isotopic composition of carbon (δ^{13}org. C, ‰) and nitrogen (δ^{15}N, ‰) of sponge species from New Zealand. Error bars indicate 1 SE.

Table 3
Results of 1-Way ANOVA to compare the biochemical composition of sponge tissue of *Tedania* sp., *Suberea meandrina*, and *Farrea raoulensis* (TC, org. C, TN), or *Tedania* sp. and *S. meandrina* (δ^{13}TC, δ^{13}org. C, δ^{15}N). Symbols: *p-value≤0.05, ⁂p-value≤0.01.

Parameter	df	F-value	p-value
TC	2	108.9	<0.0001⁂
org. C	2	69.79	<0.0001⁂
TN	2	160.4	<0.0001⁂
δ^{13}TC	1	3.414	0.138
δ^{13}org. C	1	86.78	0.0007⁂
δ^{15}N	1	1.135	0.347

± 2.27 ‰ (*F. raoulensis*, $n = 3$) (Fig. 4).

TC, org. C, and TN content of sponge tissue differed significantly between *Tedania* sp., *S. meandrina*, and *F. raoulensis* (Table 3). In contrast, the stable isotopic composition of sponge tissue differed only significantly between *Tedania* sp. and *S. meandrina* for δ^{13}org. C, but not for δ^{13}TC and δ^{15}N.

3.2. Dissolved organic matter fluxes

Sponges *Tedania* sp. and *F. raoulensis* released DOC ($5.50 \times 10^{-2} \pm 9.09 \times 10^{-2}$ µmol l^{-1} g C^{-1} d^{-1} and 11.3 ± 5.86 µmol l^{-1} g C^{-1} d^{-1}, respectively) and TDN ($0.26 \pm 5.75 \times 10^{-2}$ µmol l^{-1} g C^{-1} d^{-1} and 31.5 ± 8.22 µmol l^{-1} g C^{-1} d^{-1}, respectively), though only the TDN flux of *Tedania* sp. was significantly different from 0 (Table 4). *S. meandrina* took up DOC ($-0.12 \pm 5.16 \times 10^{-2}$ µmol l^{-1} g C^{-1} d^{-1}) and TDN (-2.49 ± 0.94 µmol l^{-1} g C^{-1} d^{-1}), again not at significant rates (Table 4).

No initial net DOC and TDN removal rates could be calculated, because the estimated parameters were not significant for any incubation (Table S3).

3.3. Fluorescent dissolved organic matter composition

The PARAFAC model could be validated for four different fluorophores (Fig. 5). Fluorophores C1 ($\lambda_{Ex} = 294$, $\lambda_{Em} = 350$) and C2 ($\lambda_{Ex} = 280$, $\lambda_{Em} = 337$) were similar to peak T and tryptophan- and protein-like (Coble, 2007, 1996). Fluorophore C3 ($\lambda_{Ex} \leq 260/332$, $\lambda_{Em} = 446$) was similar to peaks A and C and humic-like (Coble, 2007, 1996), whereas fluorophore C4 ($\lambda_{Ex} = 274$, $\lambda_{Em} = \langle 300$) was similar to peak B and tyrosine- and protein-like (Coble, 2007, 1996).

A comparison of FDOM spectra of the four fluorophores with published FDOM spectra from the "OpenFluor" online spectral library resulted in 201 comparable components (C1: 39, C2: 62, C3: 52, C4: 48) at $r_c \geq 0.95$ (Table S4).

The fluorescence intensity (R.U.) of fluorophore C1 decreased significantly over time in incubations with *S. meandrina* ($F_{1,16} = 5.77$, $p = 0.03$) (Fig. 6, Table 5). At the same time, the fluorescence intensity of fluorophores C2 and C4 increased over time [$F_{1,16}$ (C2) = 5.60, $p = 0.03$; $F_{1,16}$ (C4) = 9.17, $p = 0.008$). In comparison, the fluorescence intensity of C3 in incubations of *Tedania* sp. increased significantly over time ($F_{1,16} = 19.2$, $p = 0.0005$), whereas the fluorescence intensity of C4 in the same incubations decreased ($F_{1,16} = 4.27$, $p = 0.05$).

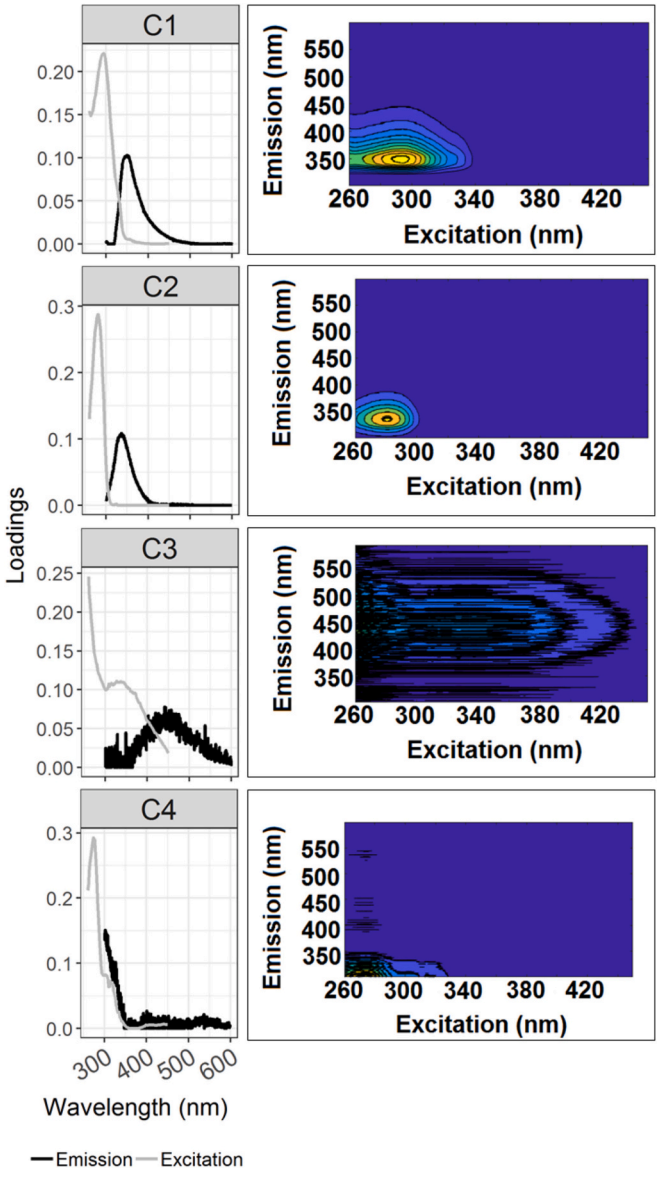

Fig. 5. Spectral loadings (Excitation/ Emission; left panels) of the fluorophores C1, C2, C3, and C4 that were identified by PARAFAC of all samples and their corresponding emission excitation scans (right panels).

3.4. Fatty acid composition of sponges

Sponges showed species-dependent differences in their PLFA compositions (Fig. 7; Table S5). Between 12.5 % (*S. meandrina*) and 46.8 % (*F. raoulensis*) of the PLFAs found in sponges consisted of long-chain fatty acids (LCFA, i.e., fatty acid with ≥24C atoms) (Fig. 7A). The other PLFA

Table 4
Results of 1-sided Student's t-tests (α = 0.05) and 1-sample Wilcoxon tests (α = 0.05) to assess whether DOC and TDN fluxes (µmol g org. C^{-1} d^{-1}) were significantly different from 0 (H_0: µ = 0, H_1: µ ≠ 0). Symbols: *p-value≤0.05, ⁂p-value≤0.01.

Sample ID	Flux type	t-value	df	V	Mean	95 % Confidence interval	p-value
Tedania sp. ($n = 3$)	DOC	0.61	2		0.056	-0.34, 0.45	0.61
	TDN	4.48	2		0.26	0.01, 0.50	0.05*
Suberea meandrina ($n = 3$)	DOC	-2.35	2		-0.12	-0.34, 0.10	0.14
	TDN			0			0.25
Farrea raoulensis ($n = 3$)	DOC	1.93	2		11.3	-13.89, 36.5	0.19
	TDN	3.83	2		31.5	-3.90, 66.9	0.06

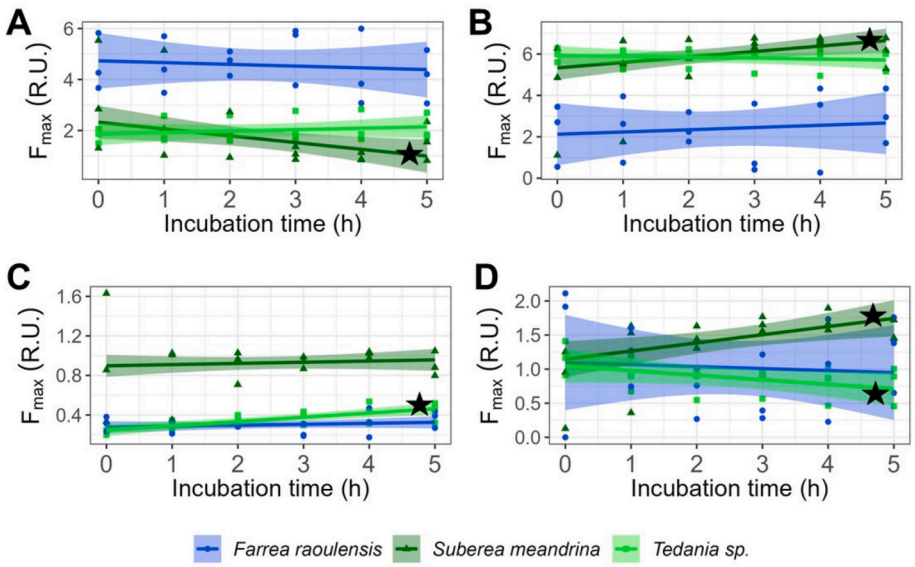

Fig. 6. Relationship of maximum fluorescence intensity F_{max} (Raman Units R.U.) to incubation time (h) for the fluorophores (A) C1, (B) C2, (C) C3, and (D) C4 that were identified in the PARAFAC model (Fig. 5).
Black stars mark robust regression analysis results that were significant at a significance level $\alpha = 0.05$ (Table 5). Shaded areas represent the 95 % confidence level intervals for the model predictions.

classes present in the sponges were branched fatty acids (4.48 ± 4.48 %), cyclic fatty acids (1.80 ± 1.12 %), highly unsaturated fatty acids (HUFA, i.e., fatty acids with ≥4 double bonds; 3.50 ± 2.89 %), methyl-fatty acids (5.44 ± 2.24 %), monosaturated fatty acids (MUFA; 18.7 ± 6.24 %), polyunsaturated fatty acids (PUFAs, i.e., fatty acids with ≥2 double bonds; 0.49 ± 0.31 %), saturated fatty acids (SFA; 22.9 ± 2.72 %), and undefined fatty acids (10.3 ± 5.66 %).

Table 5
Results of *F*-statistic (α = 0.05) of robust regression analyses to assess whether the fluorescence intensity of the identified fluorophores C1, C2, C3, and C4 (dependent or response variable) changed significantly over time (independent or predictor variable). Symbols: **p*-value≤0.05, ⁂*p*-value≤0.01, ⁂*p*-value≤0.001.

Sample ID	Incubation type	Fluorophore	*F*-statistic	df	*p*-value
Tedania sp.	Sponge	C1	0.80	1, 16	0.39
		C2	0.52	1, 16	0.48
		C3	19.2	1, 16	0.0005⁂
		C4	4.27	1, 16	0.05*
	Control	C1	2.29	1, 4	0.20
		C2	0.002	1, 4	0.97
		C3	1.06	1, 4	0.36
		C4	0.92	1, 4	0.39
Suberea meandrina	Sponge	C1	5.77	1, 16	0.03*
		C2	5.60	1, 16	0.03*
		C3	0.14	1, 16	0.71
		C4	9.17	1, 16	0.008⁑
	Control	C1	0.18	1, 3	0.70
		C2	0.03	1, 3	0.86
		C3	0.17	1, 3	0.71
		C4	1.16	1, 3	0.36
Farrea raoulensis	Sponge	C1	0.24	1, 16	0.63
		C2	0.30	1, 16	0.59
		C3	0.78	1, 16	0.39
		C4	0.10	1, 16	0.75
	Control	C1	2.00	1, 4	0.23
		C2	2.55	1, 4	0.19
		C3	0.18	1, 4	0.69
		C4	0.20	1, 4	0.68

Most isolated PLFAs were sponge-specific PLFAs (min: 13.7 % of total PLFA concentration, *S. meandrina*; max: 46.8 %, *F. raoulensis*) (Fig. 7B), followed by bacteria-specific PLFAs (min: 6.61 %, *F. raoulensis*; max: 39.1 %, *S. meandrina*), and others (min: 24.7 %, *S. meandrina*; max: 29.2 %, *Artemisina* sp.). Between 0.00 % (*Artemisina* sp.) and 20.6 % (*S. meandrina*) of the PLFAs were unidentified.

3.5. Composition of sponge-associated bacterial community

Bacterial communities of *Artemisina* sp., *S. meandrina*, and *Tedania* sp. were dominated by Proteobacteria (min: 21.7 % ASVs *S. meandrina*; max: 54.0 % ASVs *Tedania* sp.) and Chloroflexota (min: 30.1 % ASVs *S. meandrina*; max: 51.2 % ASVs *Artemisina* sp.) (Fig. 8, Table S7). The bacterial community of *F. raoulensis* was not enriched in Chloroflexota to a comparable extent, but consisted to 97.6 % of Proteobacteria. The third and fourth most abundant bacterial phyla in *S. meandrina* were Actinobacteria (14.9 % ASVs) and Acidobacteria (12.1 % ASVs) (Fig. 8).

4. Discussion

In this study, we measured DOC and TDN fluxes in shallow- and deep-water sponges and assessed whether the different sponge species transformed the FDOM composition over time. Furthermore, we tried to link the results of the FDOM analyses with fatty acid composition and the sponge-associated bacterial community to assess which role these sponges play in nutrient cycling around New Zealand.

4.1. Study limitations

Deep-sea science and particularly research expeditions are logistically challenging and often very expensive which limits type and size of experiments. As we performed the experiments on a research vessel far offshore, we were not able to acclimatize the sponges for a week before the incubations. This is possible when specimens are collected close to shore and are incubated in shore-based laboratories (e.g., Bart et al., 2021b; Wurz et al., 2024, 2021). Instead, we had to perform the experiments immediately upon retrieval of the sponges.

We aimed to fill the incubation chambers exclusively with ambient seawater that originated from the sampling site of the respective sponge

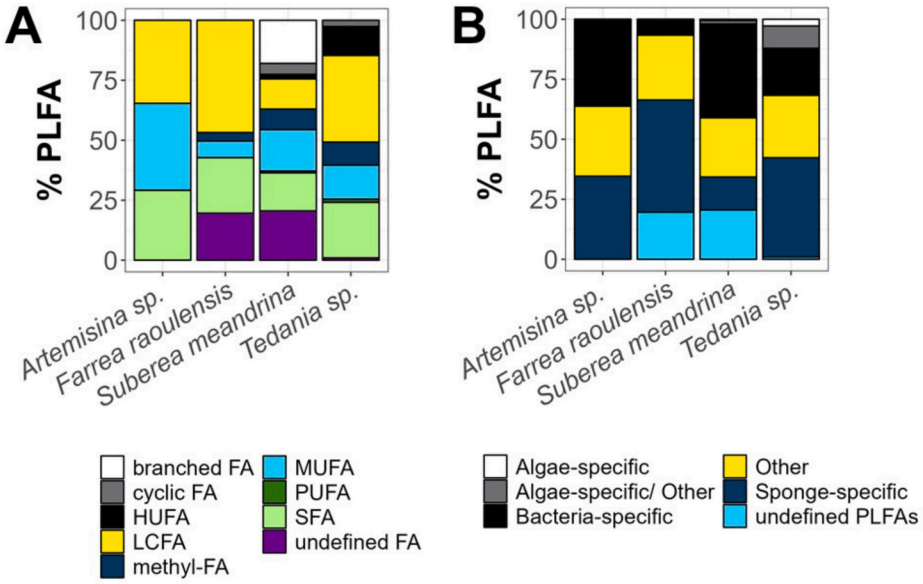

Fig. 7. (A) Contribution (%) of individual phospholipid-derived fatty acid (PLFA) classes to the total concentrations in sponges. (B) Contribution (%) of individual PLFA categories to total PLFA concentrations in sponges. Abbreviations: Branched FA = branched fatty acid, cyclic FA = cyclic fatty acid, HUFA = highly unsaturated fatty acid, LCFA = long-chain fatty acid, methyl-FA = methyl-fatty acid, MUFA = monounsaturated fatty acid, PUFA = polyunsaturated fatty acid, SFA = saturated fatty acid. Notice 'algae-specific/ other' PLFAs correspond to C20:4ω6 which co-eluted with C20:5ω3.

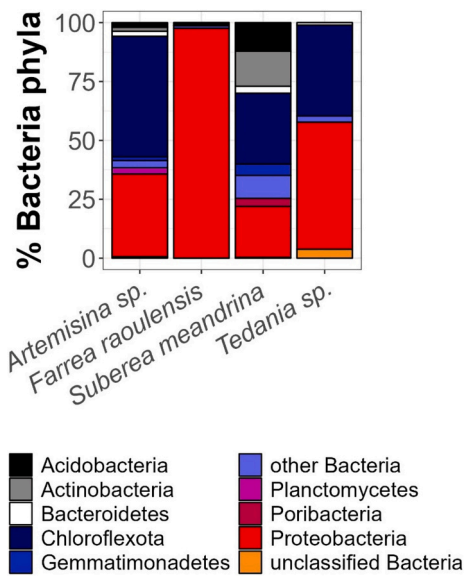

Fig. 8. Relative abundance of bacteria phyla (%) in the four sponges. The eight most abundant bacteria phyla are indicated by names, others are aggregated under the category "other Bacteria" and "unclassified Bacteria".

specimens. This, however, was not always possible and therefore we had to mix ambient seawater with seawater pumped from about 4–5 m water depth into the research vessel. Research on N cycling in deep-water hexactinellid sponges showed that these sponges can switch from consuming ammonium *in situ* to releasing it *ex situ* when they were incubated in shallower water than they lived *in situ* (Maldonado et al., 2021). Nitrate, nitrite, and phosphate fluxes seemed not be affected by this change in water quality and therefore we consider it unlikely that DOM processing was affected, but this has not been studied.

The biggest limitations of this study were the number of incubations per species and the single sample for bacteria community composition and PLFA analyses. The latter was related to post-cruise subsampling of sponge specimens for complementing studies of marine natural products. However, it would have been better to skip these additional analyses for a balanced study design.

Using only three replicates to investigate DOM cycling in deep-sea sponges seems low, but is in fact not uncommon in deep sea science (e.g. Bart et al., 2021b, 2020). Nevertheless, whenever possible, sponge incubation experiments should be performed with more replicates.

4.2. LMA/ HMA status of sponges

Based on the microbial community composition of the sponges, *F. raoulensis* is a LMA sponge with a dominance of Proteobacteria, whereas the high abundance of Acidobacteria, Actinobacteria and Chloroflexota in *S. meandrina* suggests this species may be a HMA sponge (Busch et al., 2022). Some species belonging to the genus *Tedania* have been predicted to be LMA sponges (Busch et al., 2022; Moitinho-Silva et al., 2017), but the *Tedania* sp. specimen shown here displays more of a HMA profile, with an enrichment in Chloroflexota. The *Artemisina* sp. specimen also displays a HMA profile with comparably high relative abundances of Chloroflexota.

4.3. Dissolved organic matter fluxes

Over the last 20 years, numerous studies have shown that sponges are capable of taking up DOM (e.g., Bart et al., 2020; de Goeij et al., 2013, 2008b, 2008a; Morganti et al., 2017; Ribes et al., 2023; Rix et al., 2017; Yahel et al., 2003). Initially, it was thought that only HMA sponges with their lower pumping rates and higher densities of microorganisms are able to take up DOM (Weisz et al., 2008). However, later studies showed that LMA sponges can process DOM, too (Bart et al., 2021b; Rix et al., 2020). Combining stable isotope enrichments with nanoscale secondary ion mass spectrometry (NanoSIMS), (Rix et al., 2020) showed that in HMA sponges most DOM is taken up by the microbiome. In contrast, in LMA sponges, sponge choanocytes take up most DOM, whereas the microbiome plays only a minor role in DOM processing (Rix et al., 2020).

In this study, we did not measure a significant assimilation of DOC by the HMA sponges (i.e., *S. meandrina*, *Tedania* sp., *Artemisina* sp.) nor by the LMA sponge (i.e., *F. raoulensis*), but a significant release of TDN by *Tedania* sp.

Some sponge species require a minimum DOC concentration in the ambient seawater (e.g., 79 μmol C l^{-1} seawater for *Xestospongia muta* (Schmidt, 1870) (Wooster et al., 2019); 74/80/198 μmol C l^{-1} seawater for *Agelas oroides* (Schmidt, 1864), *Crambe crambe* (Schmidt, 1862), *Chondrosia reniformis* Nardo, 1847, *Dysidea avara* (Schmidt, 1862) (Morganti et al., 2017; Ribes et al., 2023); 80 μmol C l^{-1} for *Petrosia* (*Petrosia*) *ficiformis* (Poiret, 1789) (Morganti et al., 2017)) to be able to assimilate DOM. In the incubation settings here, the initial DOC concentrations ranged from 141 to 297 μmol C l^{-1} seawater (Table S1) and therefore surpassed most of the DOC thresholds. Hence, if the sponges were capable of exploiting the DOC pool, they should have taken it up. However, the lack of significant DOC assimilation by sponges in this study compared to sponges in other studies might also be related to the inconsistent operational definition of DOC (<0.2 μm pore size vs. <0.7 μm pore size). Several studies that measured DOC consumption used a pore size of <0.7 μm (e.g., Achlatis et al., 2019; Bart et al., 2021b; de Goeij et al., 2013; Hoer et al., 2018; Morganti et al., 2017), which includes colloids and particles, whereas we used a pore size of <0.2 μm which should only allow truly dissolved DOC to pass (Verdugo et al., 2004). Hence, the sponges in this study may be unable to take up DOC or they incorporate colloidal DOC, but not truly dissolved DOC. It is also possible that the sponges took up specific DOM components and released others with no net flux of DOM.

4.4. Changes in fluorescent dissolved organic matter composition

In the incubation experiments, we identified four fluorophores by the PARAFAC model which were tryptophan- and protein like (C1, C2), humic like (C3), and tyrosine- and protein like (C4). The tryptophan-like fluorophores may be of autochthonous origin (Kellerman et al., 2015) and microbial-derived (Walker et al., 2013). They may have a low molecular weight (Wagner et al., 2015) and be part of the labile or semi-labile fraction of DOM (Davis and Benner, 2007). The humic-like fluorophore may originate from humic acids that were released during microbial processing of DOM (Stedmon and Markager, 2005; Yamashita et al., 2010) or may be generated by photo-production (Chen et al., 2010; Miranda et al., 2020). The tyrosine-like fluorophore may originate from aromatic amino acids (Yamashita and Tanoue, 2003) and be of labile or semi-labile nature (Davis and Benner, 2007) like the tryptophane-like fluorophores. These fluorophores are often degradation products (Romero et al., 2017) of small peptides or proteins (Yamashita and Tanoue, 2003).

We had expected to see a decrease in F_{max} of the different fluorophores over time as a results of DOM uptake by sponges. Instead, we measured an increase in F_{max} of fluorophores C2 (tryptophan- and protein-like), C3 (humic-like), and C4 (tyrosine- and protein-like) over time, while F_{max} of fluorophore C1 (tryptophan- and protein-like) and F_{max} of fluorophore C4 decreased. The removal of protein-like fluorophores and the release of humic-like fluorophores was reported for the Mediterranean sponges *C. reniformis*, *A. oroides*, *C. crambe*, and *D. avara*, that occasionally also excreted tryptophan-like fluorophores (Ribes et al., 2023). In fact, an untargeted metabolic analysis of exhalent and inhalant seawater samples of the sponges *Ircinia campana* (Lamarck, 1814) and *Spheciospongia vesparium* (Lamarck, 1815) from the Florida Keys (Northwestern Atlantic) detected an increase in the concentration of tryptophan and tyrosine in exhalent compared to inhalant seawater (Fiore et al., 2017). The authors even estimated that each sponge would excrete up to 1 nmol tryptophane l^{-1} seawater and 1 nmol phenylalanine l^{-1} seawater. Studies using ultrahigh-resolution mass spectrometry furthermore revealed that the sponges *Melophlus sarasinorum* Thiele, 1899, *Rhabdastrella globostellata* (Carter, 1883), and *S. vesparium* preferentially removed low-molecular mass DOM compounds (Hildebrand et al., 2022; Letourneau et al., 2020). The chemical composition of these removed compounds, however, differed between sponge species. *Melophlus sarasinorum* and *R. globostellata* targeted compounds with high C/N and high H/C ratios (Hildebrand et al., 2022), whereas *S. vesparium* depleted mainly compounds with a high N/C ratio and a low number of oxygen atoms (Letourneau et al., 2020).

4.5. Fatty acid composition of sponges

The PLFA composition of the four sponges differed quite substantially. The deep-water hexactinellid *F. raoulensis* contained seven different identified PLFAs and the shallow-water demosponges *Tedania* sp. and *S. meandrina* had a diverse range of 22 and 29 identified PLFAs, respectively. In comparison, the PFLA pool of the deep-water demosponge *Artemisina* sp. consisted of only three different PLFAs (Table S5).

The class of Hexactinellida sponges is characterized by a reduced diversity of PLFAs (Stratmann et al., 2024a; Thiel et al., 2002a), very long C chains of 28 to 32C atoms, and a lack of C chains with 24 to 28C atoms (Thiel et al., 2002a). In fact, several hexactinellids of the order Sceptrulophora which were all collected around New Zealand (this study, Stratmann et al., 2024a) showed a very close resemblance in the relative abundance of the individual PLFAs. Demosponges of the same genera that were collected in the same geographical region, however, may have very distinct PLFA profiles. (de Kluijver et al., 2021) investigated the fatty acid profiles of several boreal and Arctic demosponges of the genera *Geodia* and *Stelletta* and found that *G. barretti*, *Geodia atlantica* (Stephens, 1915), and *Geodia hentscheli* Cárdenas, Rapp, Schander & Tendal, 2010 synthesize similar LCFA in different relative abundances, whereas *Geodia parva* Hansen, 1885 and *Stelletta rhaphidiophora* Hentschel, 1929 synthesize distinct LCFA.

4.6. The role of sponges from New Zealand in nutrient cycling

By combining data about the stable isotopic composition of sponge tissue, DOC/ TDN and FDOM fluxes, microbial community composition, and PLFA composition, we tried to decipher the role of *S. meandrina*, *Tedania* sp., and *F. raoulensis* in nutrient cycling.

S. meandrina hosts bacteria of the phyla Bacteroidetes, Poribacteria, and Chloroflexota (Fig. 8, Table S7). Members of the phyla Poribacteria and Chloroflexiota, together with members of the phyla PAUC34F, Proteobacteria, and Nitrospirota are active consumers of DOM as Campana et al. (2021a) showed in a DNA-stable isotope probing experiment with the sponge *Plakortis angulospiculatus* (Carter, 1879). The authors proposed that a PAUC34f bacterium and bacteria of the genus *Endozoicomonas* (phylum Proteobacteria) were the first ones to consume and incorporate DOM, followed by a Poribacterium, a Nitrospira bacterium and three Chloroflexota bacteria. Hence, we speculate, that *S. meandrina* and particularly its dominating Chloroflexota symbionts were involved in the degradation and transformation of DOM. They degraded the tryptophan-like fluorophore C1 and/or transformed it into a fluorophore C2 with different excitation and emission maxima that still resembled a protein- or tryptophan-like fluorescence pattern (Fig. 6). At the same time, the *S. meandrina* holobiont produced a tyrosine-like fluorophore C4.

The PLFA composition of the sponge provided information about the origin of the DOM *S. meandrina* had consumed previously, as several PLFAs can serve as biomarkers (Table S6). Particularly the $\frac{C16:1\omega7}{C16:0}$-ratio indicates whether the DOM the sponge had taken up was mainly derived from diatoms ($\frac{C16:1\omega7}{C16:0} > 1$) or from dinoflagellates ($\frac{C16:1\omega7}{C16:0} < 1$) (Dalsgaard et al., 2003). *S. meandrina* had a $\frac{C16:1\omega7}{C16:0}$-ratio of 1.11 (Table S5) and therefore it likely consumed diatom-derived DOM.

The microbiome of *Tedania* sp. includes mostly Chloroflexota and Proteobacteria (Fig. 8, Table S7). In the deep-sea sponge *V. pourtalesii* Proteobacteria are involved in ammonium assimilation, ammonification, and DOM processing (Maldonado et al., 2021). Therefore, we hypothesize that *Tedania* sp. and its symbionts Chloroflexota and Proteobacteria contributed to the degradation of the tyrosine-like fluorophore C4 and the formation/ excretion of the humic-like fluorophore C3 (Fig. 6).

The DOM, which *Tedania* sp. may ammonificate to ammonium following the N cycling pathway of *Tedania* sp. from (Stratmann et al., 2024a), could have originated from highly degraded carrion or from dinoflagellates: The PLFA composition of sponge tissue contained C18:1ω9, a biomarker for highly degraded carrion-derived organic matter (Graeve et al., 2001), and C16:1ω7 and C16:0 in a $\frac{C16:1\omega7}{C16:0}$-ratio of 0.39 (Table S5) which is a biomarker for dinoflagellates (Dalsgaard et al., 2003). However, the low bulk $\delta^{15}N$ value of 5.60 ± 0.11 ‰, which is in the range of suspended POM (6.0 ± 1.9 ‰ Guo et al., 2004), pinpoints to DOM of phytoplankton-based origin; otherwise, the bulk $\delta^{15}N$ value of *Tedania* sp. would be higher.

F. raoulensis contained almost exclusively bacteria of the phyla Proteobacteria (Fig. 8, Table S7). However, in this case, Proteobacteria were likely not involved in degradation of DOM, because no significant production or consumption of DOC/ TDN/ FDOM were detected (Tables 4, 5; Fig. 6), and the PLFA composition of the sponge was dominated by long-chain fatty acids. Instead, *F. raoulensis* was characterized by a high bulk $\delta^{15}N$ value of 20.9 ± 2.27 ‰. (Hanz et al., 2022) found a similarly high $\delta^{15}N$ value of 19.4 ± 2.3 ‰ in bulk tissue of the LMA hexactinellid *Schaudinnia* sp. Schulze, 1900 from the summit of the Schulz Bank (Arctic Mid-Ocean Ridge). The authors proposed that the LMA sponges at the Schulz Bank might relay on waste products from higher trophic level consumers or on internal N recycling in the sponge tissue or in the sponge microbiome. As we did not detect DOM degradation, we hypothesize that unknown N cycling processes may occur in *F. raoulensis* which require further investigations.

5. Conclusions

In this study, we investigated the role of shallow- and deep-water sponges originating from New Zealand in the processing of DOM. *S. meandrina* takes up insignificant amounts of DOC and TDN, whereupon bacterial members of its holobiont (likely from the phyla Chloroflexota and Poribacteria) may be involved in the degradation of tryptophan-like fluorophores to a tryptophan-like fluorophore with a different chemical composition. At the same time, the sponge holobiont produces tyrosine-like fluorophores. *Tedania* sp. releases significant amounts of TDN, likely due to the production of humic-like fluorophores, while the holobiont, particularly its bacteria member Chloroflexota, may contribute to the degradation of tyrosine-like fluorophores. *F. raoulensis* does not degrade DOC or TDN, but the stable isotopic composition of its bulk tissue indicates that N recycling processes may happen inside the sponge, but these processes are so far unknown.

Funding

This research received funding from the Royal Netherlands Academy of Arts and Sciences (KNAW, The Netherlands) to TS (Academy Ecology Grant 2017) and from the Dutch Research Council (NWO, The Netherlands) to TS (NWO-Rubicon grant no. 019.182EN.012, NWO-Talent program Veni grant no. VI.Veni.212.211). AdK was supported by the SpongGES project of the European Union's Horizon 2020 research and innovation program (grant no. 679849). PS received funding by the Federal Ministry of Education and Research (BMBF) for the cruise SO254, grant no. 03G0254A, PORIBACNEWZ.

Specimens were collected as part of the project "PoriBacNewZ" by the Institut für Chemie und Biologie des Meeres (ICBM), University Oldenburg on the German flagship RV *Sonne*, using the ROV Kiel 6000 (GEOMAR) with participation and funding from GEOMAR, DSMZ, LMU, NIOZ, NIWA, and ETH-Zurich. NIWA voyage participation was funded through the MBIE SSIF Enhancing Collections project.

CRediT authorship contribution statement

Tanja Stratmann: Writing – original draft, Visualization, Validation, Software, Resources, Project administration, Methodology, Investigation, Funding acquisition, Formal analysis, Data curation, Conceptualization. **Mario L.M. Miranda:** Writing – review & editing, Methodology, Investigation, Formal analysis. **Anna de Kluijver:** Methodology, Investigation. **Kathrin Busch:** Writing – review & editing, Methodology, Investigation, Data curation. **Michelle Kelly:** Writing – review & editing, Formal analysis. **Sadie Mills:** Writing – review & editing, Validation, Resources, Data curation. **Peter J. Schupp:** Writing – review & editing, Supervision, Resources, Funding acquisition.

Declaration of competing interest

There are no conflicts of interest declared for this submission.

Acknowledgements

The authors thank chief scientist Prof. Meinhard Simon (University of Oldenburg), the captain and crew of RV *Sonne*, and the ROV Kiel 6000 team from Geomar (Kiel) for their excellent support during research cruise SO254. The authors acknowledge the analytical support from Peter van Breugel (NIOZ) and from Klaas Nierop (Utrecht University). They further acknowledge Thorsten Dittmar, Ina Ulber, and Matthias Friebe (University of Oldenburg) for conducting the TDN/ DOC analyses. Dick van Oevelen (NIOZ) is thanked for providing funding for shipment of equipment to New Zealand.

Appendix A. Supplementary data

Supplementary data to this article can be found online at https://doi.org/10.1016/j.jembe.2025.152092.

Data availability

All data presented in this manuscript are available at Pangaea (doi: 10.1594/PANGAEA.971543, doi: 10.1594/PANGAEA.971544) and on NCBI (accession numbers: PRJNA1102912; http://www.ncbi.nlm.nih.gov/bioproject/1102912). Sample collection was carried out under the "Application for consent to conduct marine scientific research in areas under national jurisdiction of New Zealand (dated 07.06.2016)." Sponge collection at Raoul Island was performed under the "Authorization to undertake specified scientific study within a marine reserve" (authorization number: 53535-MAR, dated 22.12.2016).

References

Achlatis, M., Pernice, M., Green, K., De Goeij, J.M., Guagliardo, P., Kilburn, M.R., Hoegh-Guldberg, O., Dove, S., 2019. Single-cell visualization indicates direct role of sponge host in uptake of dissolved organic matter. Proc. R. Soc. B Biol. Sci. 286, 20192153. https://doi.org/10.1098/rspb.2019.2153.

Alexander, B.E., Liebrand, K., Osinga, R., van der Geest, H.G., Admiraal, W., Cleutjens, J. P.M., Schutte, B., Verheyen, F., Ribes, M., van Loon, E., de Goeij, J.M., 2014. Cell turnover and detritus production in marine sponges from tropical and temperate benthic ecosystems. PloS One 9, e109486. https://doi.org/10.1371/journal.pone.0109486.

Andersson, C.A., Bro, R., 2000. The N-way toolbox for MATLAB. Chemom. Intel. Lab. Syst. 52, 1–4. https://doi.org/10.1016/S0169-7439(00)00071-X.

Archer, S.K., Stevens, J.L., Rossi, R.E., Matterson, K.O., Layman, C.A., 2017. Abiotic conditions drive significant variability in nutrient processing by a common Caribbean sponge, *Ircinia felix*. Limnol. Oceanogr. 62, 1783–1793. https://doi.org/10.1002/lno.10533.

Barnes, D.K.A., 1999. High diversity of tropical intertidal zone sponges in temperature, salinity and current extremes. Afr. J. Ecol. 37, 424–434. https://doi.org/10.1046/j.1365-2028.1999.00197.x.

Bart, M.C., de Kluijver, A., Hoetjes, S., Absalah, S., Mueller, B., Kenchington, E., Rapp, H. T., de Goeij, J.M., 2020. Differential processing of dissolved and particulate organic matter by deep-sea sponges and their microbial symbionts. Sci. Rep. 10, 17515. https://doi.org/10.1038/s41598-020-74670-0.

Bart, M.C., Hudspith, M., Rapp, H.T., Verdonschot, P.F.M., de Goeij, J.M., 2021a. A deep-sea sponge loop? Sponges transfer dissolved and particulate organic carbon and nitrogen to associated fauna. Front. Mar. Sci. 8, 604879. https://doi.org/10.3389/fmars.2021.604879.

Bart, M.C., Mueller, B., Rombouts, T., van de Ven, C., Tompkins, G.J., Osinga, R., Brussaard, C.P.D., MacDonald, B., Engel, A., Rapp, H.T., de Goeij, J.M., 2021b. Dissolved organic carbon (DOC) is essential to balance the metabolic demands of four dominant North-Atlantic deep-sea sponges. Limnol. Oceanogr. 66, 925–938. https://doi.org/10.1002/lno.11652.

Bauer, J.E., Williams, P.M., Druffel, E.R.M., 1992. 14C activity of dissolved organic carbon fractions in the north-central Pacific and Sargasso Sea. Nature 357, 667–670. https://doi.org/10.1038/357667a0.

Beaulieu, S.E., 2001. Life on glass houses: sponge stalk communities in the deep sea. Mar. Biol. 138, 803–817. https://doi.org/10.1007/s002270000500.

Belmonte, T., Alvim, J., Padula, V., Muricy, G., 2015. Spongivory by nudibranchs on the coast of Rio de Janeiro state, southeastern Brazil (Mollusca, Gastropoda). Spixiana 2, 187–195.

Bligh, E.G., Dyer, W.J., 1959. A rapid method of total lipid extraction and purification. Can. J. Biochem. Physiol. 37, 911–917. https://doi.org/10.1139/o59-099.

Bolyen, E., Rideout, J.R., Dillon, M.R., Bokulich, N.A., Abnet, C.C., Al-Ghalith, G.A., Alexander, H., Alm, E.J., Arumugam, M., Asnicar, F., Bai, Y., Bisanz, J.E., Bittinger, K., Brejnrod, A., Brislawn, C.J., Brown, C.T., Callahan, B.J., Caraballo-Rodríguez, A.M., Chase, J., Cope, E.K., Da Silva, R., Diener, C., Dorrestein, P.C., Douglas, G.M., Durall, D.M., Duvallet, C., Edwardson, C.F., Ernst, M., Estaki, M., Fouquier, J., Gauglitz, J.M., Gibbons, S.M., Gibson, D.L., Gonzalez, A., Gorlick, K., Guo, J., Hillmann, B., Holmes, S., Holste, H., Huttenhower, C., Huttley, G.A., Janssen, S., Jarmusch, A.K., Jiang, L., Kaehler, B.D., Kang, K. Bin, Keefe, C.R., Keim, P., Kelley, S.T., Knights, D., Koester, I., Kosciolek, T., Kreps, J., Langille, M.G. I., Lee, J., Ley, R., Liu, Y.-X., Loftfield, E., Lozupone, C., Maher, M., Marotz, C., Martin, B.D., McDonald, D., McIver, L.J., Melnik, A.V., Metcalf, J.L., Morgan, S.C., Morton, J.T., Naimey, A.T., Navas-Molina, J.A., Nothias, L.F., Orchanian, S.B., Pearson, T., Peoples, S.L., Petras, D., Preuss, M.L., Pruesse, E., Rasmussen, L.B., Rivers, A., Robeson, M.S., Rosenthal, P., Segata, N., Shaffer, M., Shiffer, A., Sinha, R., Song, S.J., Spear, J.R., Swafford, A.D., Thompson, L.R., Torres, P.J., Trinh, P., Tripathi, A., Turnbaugh, P.J., Ul-Hasan, S., van der Hooft, J.J.J., Vargas, F., Vázquez-Baeza, Y., Vogtmann, E., von Hippel, M., Walters, W., Wan, Y., Wang, M., Warren, J., Weber, K.C., Williamson, C.H.D., Willis, A.D., Xu, Z.Z., Zaneveld, J.R., Zhang, Y., Zhu, Q., Knight, R., Caporaso, J.G., 2019. Reproducible, interactive, scalable and extensible microbiome data science using QIIME 2. Nat. Biotechnol. 37, 852–857. https://doi.org/10.1038/s41587-019-0209-9.

Bro, R., 1998. Multi-Way Analysis in the Food Industry: Models, Algorithms and Applications. PhD-Thesis. Universiteit van Amsterdam.

Busch, K., Slaby, B.M., Bach, W., Boetius, A., Clefsen, I., Colaço, A., Creemers, M., Cristobo, J., Federwisch, L., Franke, A., Gavriilidou, A., Hethke, A., Kenchington, E., Mienis, F., Mills, S., Riesgo, A., Ríos, P., Roberts, E.M., Sipkema, D., Pita, L., Schupp, P.J., Xavier, J., Rapp, H.T., Hentschel, U., 2022. Biodiversity, environmental drivers, and sustainability of the global deep-sea sponge microbiome. Nat. Commun. 13, 5160. https://doi.org/10.1038/s41467-022-32684-4.

Callahan, B.J., McMurdie, P.J., Rosen, M.J., Han, A.W., Johnson, A.J.A., Holmes, S.P., 2016. DADA2: high-resolution sample inference from Illumina amplicon data. Nat. Methods 13, 581–583. https://doi.org/10.1038/nmeth.3869.

Campana, S., Busch, K., Hentschel, U., Muyzer, G., de Goeij, J.M., 2021a. DNA-stable isotope probing (DNA-SIP) identifies marine sponge-associated bacteria actively utilizing dissolved organic matter (DOM). Environ. Microbiol. 23, 4489–4504. https://doi.org/10.1111/1462-2920.15642.

Campana, S., Hudspith, M., Lankes, D., de Kluijver, A., Demey, C., Schoorl, J., Absalah, S., van der Meer, M.T.J., Mueller, B., de Goeij, J.M., 2021b. Processing of naturally sourced macroalgal- and coral-dissolved organic matter (DOM) by high and low microbial abundance encrusting sponges. Front. Mar. Sci. 8. https://doi.org/10.3389/fmars.2021.640583.

Caporaso, J.G., Lauber, C.L., Walters, W.A., Berg-Lyons, D., Lozupone, C.A., Turnbaugh, P.J., Fierer, N., Knight, R., 2011. Global patterns of 16S rRNA diversity at a depth of millions of sequences per sample. Proc. Natl. Acad. Sci. U. S. A. 108, 4516–4522. https://doi.org/10.1073/pnas.1000080107.

Carballeira, N., Thompson, J.E., Ayanoglu, E., Djerassi, C., 1986. Biosynthetic studies of marine lipids. 5. The biosynthesis of long-chain branched fatty acids in marine sponges. J. Org. Chem. 51, 2751–2756. https://doi.org/10.1021/jo00364a024.

Cathalot, C., Van Oevelen, D., Cox, T.J.S., Kutti, T., Lavaleye, M., Duineveld, G.C.A., Meysman, F.J.R., 2015. Cold-water coral reefs and adjacent sponge grounds: hotspots of benthic respiration and organic carbon cycling in the deep sea. Front. Mar. Sci. 2, 1–12. https://doi.org/10.3389/fmars.2015.00037.

Chen, M., Price, R.M., Yamashita, Y., Jaffé, R., 2010. Comparative study of dissolved organic matter from groundwater and surface water in the Florida coastal Everglades using multi-dimensional spectrofluorometry combined with multivariate statistics. Appl. Geochem. 25, 872–880. https://doi.org/10.1016/j.apgeochem.2010.03.005.

Chu, J., Leys, S., 2010. High resolution mapping of community structure in three glass sponge reefs (Porifera, Hexactinellida). Mar. Ecol. Prog. Ser. 417, 97–113. https://doi.org/10.3354/meps08794.

Coble, P.G., 1996. Characterization of marine and terrestrial DOM in seawater using excitation-emission matrix spectroscopy. Mar. Chem. 51, 325–346. https://doi.org/10.1016/0304-4203(95)00062-3.

Coble, P.G., 2007. Marine optical biogeochemistry: the chemistry of ocean color. Chem. Rev. 107, 402–418. https://doi.org/10.1021/cr050350+.

Conway, K.W., Krautter, M., Vaughn Barrie, J., Neuwciler, M., 2001. Hexactinellid sponge reefs on the Canadian continental shelf: a unique "living fossil.". Geosci. Can. 28, 71–78.

Dahihande, A.S., Thakur, N.L., 2019. Temperature- and size-associated differences in the skeletal structures and osculum cross-sectional area influence the pumping rate of contractile sponge *Cinachyrella* cf. *cavernosa*. Mar. Ecol. 40, e12565. https://doi.org/10.1111/maec.12565.

Dalsgaard, J., St. John, M., Kattner, G., Müller-Navarra, D., Hagen, W., 2003. Fatty acid trophic markers in the pelagic marine environment. Adv. Mar. Biol. 46, 225–340. https://doi.org/10.1016/S0065-2881(03)46005-7.

Davis, J., Benner, R., 2007. Quantitative estimates of labile and semi-labile dissolved organic carbon in the western Arctic Ocean: a molecular approach. Limnol. Oceanogr. 52, 2434–2444. https://doi.org/10.4319/lo.2007.52.6.2434.

de Goeij, J.M., van Duyl, F.C., 2007. Coral cavities are sinks of dissolved organic carbon (DOC). Limnol. Oceanogr. 52, 2608–2617. https://doi.org/10.4319/lo.2007.52.6.2608.

de Goeij, J.M., Moodley, L., Houtekamer, M., Carballeira, N.M., van Duyl, F.C., 2008a. Tracing 13C-enriched dissolved and particulate organic carbon in the bacteria-containing coral reef sponge Halisarca caerulea: evidence for DOM-feeding. Limnol. Oceanogr. 53, 1376–1386. https://doi.org/10.4319/lo.2008.53.4.1376.

de Goeij, J.M., van den Berg, H., van Oostveen, M.M., Epping, E., van Duyl, F.C., 2008b. Major bulk dissolved organic carbon (DOC) removal by encrusting coral reef cavity sponges. Mar. Ecol. Prog. Ser. 357, 139–151. https://doi.org/10.3354/meps07403.

de Goeij, J.M., van Oevelen, D., Vermeij, M.J.A., Osinga, R., Middelburg, J.J., de Goeij, A.F.P.M., Admiraal, W., 2013. Surviving in a marine desert: the sponge loop retains resources within coral reefs. Science 1979 (342), 108–110. https://doi.org/10.1126/science.1241981.

De Goeij, J.M., Lesser, M.P., Pawlik, J.R., 2017. Nutrient fluxes and ecological functions of coral reef sponges in a changing ocean. In: Climate Change, Ocean Acidification and Sponges: Impacts across Multiple Levels of Organization. Springer International Publishing, pp. 373–410. https://doi.org/10.1007/978-3-319-59008-0_8.

de Kluijver, A., 2021. Fatty acid analysis sponges. protocols.io. https://doi.org/10.17504/protocols.io.bhnpj5dn.

de Kluijver, A., Nierop, K.G.J., Morganti, T.M., Bart, M.C., Slaby, B.M., Hanz, U., de Goeij, J.M., Mienis, F., Middelburg, J.J., 2021. Bacterial precursors and unsaturated long-chain fatty acids are biomarkers of North-Atlantic deep-sea demosponges. PloS One 16, e0241095. https://doi.org/10.1371/journal.pone.0241095.

Diaz, M.C., Rützler, K., 2001. Sponges: an essential component of Caribbean coral reefs. Bull. Mar. Sci. 69, 535–546.

Dohrmann, M., Reiswig, H.M., Kelly, M., Mills, S., Schätzle, S., Reverter, M., Niesse, N., Rohde, S., Schupp, P., Wörheide, G., 2023. Expanded sampling of New Zealand glass sponges (Porifera: Hexactinellida) provides new insights into biodiversity, chemodiversity, and phylogeny of the class. PeerJ 11. https://doi.org/10.7717/peerj.15017.

Downey, R.V., Griffiths, H.J., Linse, K., Janussen, D., 2012. Diversity and distribution patterns in high southern latitude sponges. PloS One 7. https://doi.org/10.1371/journal.pone.0041672.

Druffel, E.R.M., Griffin, S., Wang, N., Garcia, N.G., McNichol, A.P., Key, R.M., Walker, B. D., 2019. Dissolved organic radiocarbon in the central Pacific Ocean. Geophys. Res. Lett. 46, 5396–5403. https://doi.org/10.1029/2019GL083149.

Dunham, A., Archer, S.K., Davies, S.C., Burke, L.A., Mossman, J., Pegg, J.R., Archer, E., 2018. Assessing condition and ecological role of deep-water biogenic habitats: glass sponge reefs in the Salish Sea. Mar. Environ. Res. 141, 88–99. https://doi.org/10.1016/j.marenvres.2018.08.002.

Dunlap, M., Pawlik, J.R., 1998. Spongivory by parrotfish in Florida mangrove and reef habitats. Mar. Ecol. 19, 325–337. https://doi.org/10.1111/j.1439-0485.1998.tb00471.x.

Elzhov, T.V., Mullen, K.M., Spiess, A.-N., Bolker, B., 2023. R Interface to the Levenberg-Marquardt Nonlinear Least-Squares Algorithm Found in MINPACK, Plus Support for Bounds.

Erwin, P.M., Coma, R., López-Sendino, P., Serrano, E., Ribes, M., 2015. Stable symbionts across the HMA-LMA dichotomy: Low seasonal and interannual variation in sponge-associated bacteria from taxonomically diverse hosts. FEMS Microbiol. Ecol. 91, fiv115. https://doi.org/10.1093/femsec/fiv115.

Fiore, C.L., Freeman, C.J., Kujawinski, E.B., 2017. Sponge exhalent seawater contains a unique chemical profile of dissolved organic matter. PeerJ 5, e2870. https://doi.org/10.7717/peerj.2870.

Fuhrmann, J.A., Ferguson, R.L., 1986. Nanomolar concentrations and rapid turnover of dissolved free amino acids in seawater: agreement between chemical and microbiological measurements. Mar. Ecol. Prog. Ser. 33, 237–242.

Gastaldi, M., De Paula, T.S., Narvarte, M.A., Lôbo-Hajdu, G., Hajdu, E., 2018. Marine sponges (Porifera) from the Bahía San Antonio (North Patagonian Gulfs, Argentina), with additions to the phylogeography of the widely distributed *Cliona* aff. *celata* and *Hymeniacidon perlevis*, and the description of two new species. Mar. Biol. Res. 14, 682–716. https://doi.org/10.1080/17451000.2018.1506136.

Giles, E.C., Kamke, J., Moitinho-Silva, L., Taylor, M.W., Hentschel, U., Ravasi, T., Schmitt, S., 2013. Bacterial community profiles in low microbial abundance sponges. FEMS Microbiol. Ecol. 83, 232–241. https://doi.org/10.1111/j.1574-6941.2012.01467.x.

Graeve, M., Dauby, P., Scailteur, Y., 2001. Combined lipid, fatty acid and digestive tract content analyses: a penetrating approach to estimate feeding modes of Antarctic amphipods. Polar Biol. 24, 853–862. https://doi.org/10.1007/s003000100295.

Guo, L., Tanaka, T., Wang, D., Tanaka, N., Murata, A., 2004. Distributions, speciation and stable isotope composition of organic matter in the southeastern Bering Sea. Mar. Chem. 91, 211–226. https://doi.org/10.1016/j.marchem.2004.07.002.

Hadas, E., Shpigel, M., Ilan, M., 2009. Particulate organic matter as a food source for a coral reef sponge. J. Exp. Biol. 212, 3643–3650. https://doi.org/10.1242/jeb.027953.

Halewood, E., Opalk, K., Custals, L., Carey, M., Hansell, D.A., Carlson, C.A., 2022. Determination of dissolved organic carbon and total dissolved nitrogen in seawater using High Temperature Combustion Analysis. Front. Mar. Sci. 9. https://doi.org/10.3389/fmars.2022.1061646.

Hansell, D.A., Carlson, C.A., Repeta, D.J., Schlitzer, R., 2009. Dissolved organic matter in the ocean: a controversy stimulates new insights. Oceanography 22, 202–211. https://doi.org/10.5670/oceanog.2009.109.

Hansell, D.A., Carlson, C.A., Schlitzer, R., 2012. Net removal of major marine dissolved organic carbon fractions in the subsurface ocean. Global Biogeochem. Cycles 26. https://doi.org/10.1029/2011GB004069.

Hanz, U., Riekenberg, P., de Kluijver, A., van der Meer, M., Middelburg, J.J., de Goeij, J. M., Bart, M.C., Wurz, E., Colaço, A., Duineveld, G.C.A., Reichart, G.J., Rapp, H.T., Mienis, F., 2022. The important role of sponges in carbon and nitrogen cycling in a deep-sea biological hotspot. Funct. Ecol. 36, 2188–2199. https://doi.org/10.1111/1365-2435.14117.

Hawkes, N., Korabik, M., Beazley, L., Rapp, H.T., Xavier, J.R., Kenchington, E., 2019. Glass sponge grounds on the Scotian shelf and their associated biodiversity. Mar. Ecol. Prog. Ser. 614, 91–109. https://doi.org/10.3354/meps12903.

Hentschel, U., Usher, K.M., Taylor, M.W., 2006. Marine sponges as microbial fermenters. FEMS Microbiol. Ecol. 55, 167–177. https://doi.org/10.1111/j.1574-6941.2005.00046.x.

Hestetun, J.T., Vacelet, J., Boury-Esnault, N., Borchiellini, C., Kelly, M., Ríos, P., Cristobo, J., Rapp, H.T., 2016. The systematics of carnivorous sponges. Mol. Phylogenet. Evol. 94, 327–345. https://doi.org/10.1016/j.ympev.2015.08.022.

Hildebrand, T., Osterholz, H., Bunse, C., Grotheer, H., Dittmar, T., Schupp, P.J., 2022. Transformation of dissolved organic matter by two Indo-Pacific sponges. Limnol. Oceanogr. 67, 2483–2496. https://doi.org/10.1002/lno.12214.

Hoer, D.R., Tommerdahl, J.P., Lindquist, N.L., Martens, C.S., 2018. Dissolved inorganic nitrogen fluxes from common Florida Bay (U.S.A.) sponges. Limnol. Oceanogr. 63, 2563–2578. https://doi.org/10.1002/lno.10960.

Kaneda, T., 1991. Iso-and anteiso-fatty acids in bacteria: biosynthesis, function, and taxonomic significance. Microbiol. Rev. 55, 288–302.

Keil, R.G., Kirchman, D.L., 1999. Utilization of dissolved protein and amino acids in the northern Sargasso Sea. Aquat. Microb. Ecol. 18, 293–300.

Kellerman, A.M., Kothawala, D.N., Dittmar, T., Tranvik, L.J., 2015. Persistence of dissolved organic matter in lakes related to its molecular characteristics. Nat. Geosci. 8, 454–457. https://doi.org/10.1038/ngeo2440.

Kelly, M., Sim-Smith, C., 2023. Kingdom Animalia, phylum Porifera (sponges). In: Kelly, M., Mills, S., Terezow, M., Sim-Smith, C., Nelson, W. (Eds.), The Marine Biota of Aotearoa New Zealand. Updating Our Marine Biodiversity Inventory, NIWA Biodiversity Memoir, pp. 84–109.

Kersken, D., Göcke, C., Brandt, A., Lejzerowicz, F., Schwabe, E., Anna Seefeldt, M., Veit-Köhler, G., Janussen, D., 2014. The infauna of three widely distributed sponge species (Hexactinellida and Demospongiae) from the deep Ekström Shelf in the Weddell Sea, Antarctica. Deep-Sea Res. II 108, 101–112. https://doi.org/10.1016/j.dsr2.2014.06.005.

Kersken, D., Janussen, D., Arbizu, P.M., 2019. Deep-sea glass sponges (Hexactinellida) from polymetallic nodule fields in the Clarion-Clipperton Fracture Zone (CCFZ), northeastern Pacific: part II – Hexasterophora. Mar. Biodivers. 49, 947–987. https://doi.org/10.1007/s12526-018-0880-y.

Lakowicz, J., 2006. Principles of Fluorescence Spectroscopy, 3rd ed. Springer Science+Business Media, LLC, New York.

Letourneau, M.L., Hopkinson, B.M., Fitt, W.K., Medeiros, P.M., 2020. Molecular composition and biodegradation of loggerhead sponge *Spheciospongia vesparium* exhalent dissolved organic matter. Mar. Environ. Res. 162. https://doi.org/10.1016/j.marenvres.2020.105130.

Leys, S.P., Yahel, G., Reidenbach, M.A., Tunnicliffe, V., Shavit, U., Reiswig, H.M., 2011. The sponge pump: the role of current induced flow in the design of the sponge body plan. PloS One 6, e27787. https://doi.org/10.1371/journal.pone.0027787.

Lorenzo-Seva, U., ten Berge, J.M.F., 2006. Tucker's congruence coefficient as a meaningful index of factor similarity. Methodology 2, 57–64. https://doi.org/10.1027/1614-2241.2.2.57.

Maier, S.R., Kutti, T., Bannister, R.J., Fang, J.K.-H., van Breugel, P., van Rijswijk, P., van Oevelen, D., 2020. Recycling pathways in cold-water coral reefs: use of dissolved organic matter and bacteria by key suspension feeding taxa. Sci. Rep. 10, 9942. https://doi.org/10.1038/s41598-020-66463-2.

Maldonado, M., Aguilar, R., Bannister, R.J., Bell, J.J., Conway, K.W., Dayton, P.K., Diaz, C., Gutt, J., Kelly, M., Kenchington, E.L.R., Leys, S.P., Pomponi, S.A., Tendal, Ole S., Rapp, H.T., Rützler, K., Tendal, Ole Secher, Vacelet, J., Young, C.M., 2017. Sponge grounds as key marine habitats: A synthetic review of types, structure, functional roles, and conservation concerns. In: Marine Animal Forests. Springer International Publishing, Cham. https://doi.org/10.1007/978-3-319-17001-5.

Maldonado, M., López-Acosta, M., Busch, K., Slaby, B.M., Bayer, K., Beazley, L., Hentschel, U., Kenchington, E., Rapp, H.T., 2021. A microbial nitrogen engine modulated by Bacteriosyncytia in hexactinellid sponges: ecological implications for deep-sea communities. Front. Mar. Sci. 8, 638505. https://doi.org/10.3389/fmars.2021.638505.

Massaro, A.J., Weisz, J.B., Hill, M.S., Webster, N.S., 2012. Behavioral and morphological changes caused by thermal stress in the Great Barrier Reef sponge *Rhopaloeides odorabile*. J. Exp. Mar. Biol. Ecol. 416–417, 55–60. https://doi.org/10.1016/j.jembe.2012.02.008.

McIntyre, F.D., Drewery, J., Eerkes-Medrano, D., Neat, F.C., 2016. Distribution and diversity of deep-sea sponge grounds on the Rosemary Bank Seamount, NE Atlantic. Mar. Biol. 163. https://doi.org/10.1007/s00227-016-2913-z.

McMurray, S.E., Johnson, Z.I., Hunt, D.E., Pawlik, J.R., Finelli, C.M., 2016. Selective feeding by the giant barrel sponge enhances foraging efficiency. Limnol. Oceanogr. 61, 1271–1286. https://doi.org/10.1002/lno.10287.

McMurray, S., Stubler, A., Erwin, P., Finelli, C., Pawlik, J., 2018. A test of the sponge-loop hypothesis for emergent Caribbean reef sponges. Mar. Ecol. Prog. Ser. 588, 1–14. https://doi.org/10.3354/meps12466.

Meylan, A., 1988. Spongivory in hawksbill turtles: a diet of glass. Science 1979 (239), 393–395. https://doi.org/10.1126/science.239.4838.393.

Miranda, M.L., Osterholz, H., Giebel, H.A., Bruhnke, P., Dittmar, T., Zielinski, O., 2020. Impact of UV radiation on DOM transformation on molecular level using FT-ICR-MS and PARAFAC. Spectrochim. Acta A Mol. Biomol. Spectrosc. 230. https://doi.org/10.1016/j.saa.2020.118027.

Moitinho-Silva, L., Steinert, G., Nielsen, S., Hardoim, C.C.P., Wu, Y.C., McCormack, G.P., López-Legentil, S., Marchant, R., Webster, N., Thomas, T., Hentschel, U., 2017. Predicting the HMA-LMA status in marine sponges by machine learning. Front. Microbiol. 8, 752. https://doi.org/10.3389/fmicb.2017.00752.

Moré, J.J., 1978. The Levenberg-Marquardt algorithm: implementation and theory. In: Watson, G.A. (Ed.), Numerical Analysis, Lecture Notes in Mathematics. Springer, Berlin, Heidelberg, pp. 105–116. https://doi.org/10.1007/BFb0067700.

Morganti, T., Coma, R., Yahel, G., Ribes, M., 2017. Trophic niche separation that facilitates co-existence of high and low microbial abundance sponges is revealed by in situ study of carbon and nitrogen fluxes. Limnol. Oceanogr. 62, 1963–1983. https://doi.org/10.1002/lno.10546.

Morganti, T.M., Purser, A., Rapp, H.T., German, C.R., Jakuba, M.V., Hehemann, L., Blendl, J., Slaby, B.M., Boetius, A., 2021. *In situ* observation of sponge trails suggests common sponge locomotion in the deep central Arctic. Curr. Biol. 31, R368–R370. https://doi.org/10.1016/j.cub.2021.03.014.

Morganti, T.M., Slaby, B.M., de Kluijver, A., Busch, K., Hentschel, U., Middelburg, J.J., Grotheer, H., Mollenhauer, G., Dannheim, J., Rapp, H.T., Purser, A., Boetius, A., 2022. Giant sponge grounds of Central Arctic seamounts are associated with extinct seep life. Nat. Commun. 13, 638. https://doi.org/10.1038/s41467-022-28129-7.

Murphy, K.R., Stedmon, C.A., Graeber, D., Bro, R., 2013. Fluorescence spectroscopy and multi-way techniques. PARAFAC. Analytical Methods 5, 6557–6566. https://doi.org/10.1039/c3ay41160e.

Murphy, K.R., Stedmon, C.A., Wenig, P., Bro, R., 2014. OpenFluor- an online spectral library of auto-fluorescence by organic compounds in the environment. Anal. Methods 6, 658–661. https://doi.org/10.1039/C3AY41935E.

Muyzer, G., De Waal, E.C., Uitierlinden, A.G., 1993. Profiling of complex microbial populations by denaturing gradient gel electrophoresis analysis of polymerase chain reaction-amplified genes coding for 16S rRNA. In: Applied and Environmental Microbiology.

Pawlik, J.R., McMurray, S.E., 2020. The emerging ecological and biogeochemical importance of sponges on coral reefs. Ann. Rev. Mar. Sci. 12, 315–337. https://doi.org/10.1146/annurev-marine-010419-010807.

Quast, C., Pruesse, E., Yilmaz, P., Gerken, J., Schweer, T., Yarza, P., Peplies, J., Glöckner, F.O., 2013. The SILVA ribosomal RNA gene database project: improved data processing and web-based tools. Nucleic Acids Res. 41. https://doi.org/10.1093/nar/gks1219.

Ramirez-Llodra, E., Meyer, H.K., Bluhm, B.A., Brix, S., Brandt, A., Dannheim, J., Downey, R.V., Egilsdóttir, H., Eilertsen, M.H., Gaudron, S.M., Gebruk, A., Golikov, A., Hasemann, C., Hilario, A., Jørgensen, L.L., Kaiser, S., Korfhage, S.A., Kürzel, K., Lörz, A.-N., Buhl-Mortensen, P., Olafsdóttir, S.H., Piepenburg, D., Purser, A., Ribeiro, P.A., Sen, A., Soltwedel, T., Stratmann, T., Steger, J., Svavarsson, J., Tandberg, A.H.S., Taylor, J., Theising, F.I., Uhlir, C., Waller, R.G., Xavier, J.R., Zhulay, I., Saaedi, H., 2024. The emerging picture of a diverse deep Arctic Ocean seafloor: from habitats to ecosystems. Elem. Sci. Anth. 12, 1–38. https://doi.org/10.1525/elementa.2023.00140.

Ramiro-Sánchez, B., González-Irusta, J.M., Henry, L.-A., Cleland, J., Yeo, I., Xavier, J.R., Carreiro-Silva, M., Sampaio, Í., Spearman, J., Victorero, L., Messing, C.G., Kazanidis, G., Roberts, J.M., Murton, B., 2019. Characterization and mapping of a deep-sea sponge ground on the tropic seamount (northeast tropical Atlantic): implications for spatial management in the high seas. Front. Mar. Sci. 6, 278. https://doi.org/10.3389/fmars.2019.00278.

R-Core Team, 2022. R: A Language and Environment for Statistical Computing.

Reiswig, H.M., Dohrmann, M., Kelly, M., Mills, S., Schupp, P.J., Wörheide, G., 2021. Rossellid glass sponges (Porifera, hexactinellida) from New Zealand waters, with description of one new genus and six new species. Zookeys 2021, 33–84. https://doi.org/10.3897/zookeys.1060.63307.

Repeta, D.J., 2015. Chemical characterization and cycling of dissolved organic matter. In: Hansell, D.A., Carlson, C.A. (Eds.), Biogeochemistry of Marine Dissolved Organic Matter. Elsevier Inc., Amsterdam, pp. 21–63. https://doi.org/10.1016/B978-0-12-405940-5.00002-9.

Ribes, M., Yahel, G., Romera-Castillo, C., Mallenco, R., Morganti, T.M., Coma, R., 2023. The removal of dissolved organic matter by marine sponges is a function of its composition and concentration: an in situ seasonal study of four Mediterranean species. Sci. Total Environ. 871. https://doi.org/10.1016/j.scitotenv.2023.161991.

Rix, L., de Goeij, J.M., Mueller, C.E., Struck, U., Middelburg, J.J., van Duyl, F.C., Al-Horani, F.A., Wild, C., Naumann, M.S., van Oevelen, D., 2016. Coral mucus fuels the sponge loop in warm- and cold-water coral reef ecosystems. Sci. Rep. 6, 18715. https://doi.org/10.1038/srep18715.

Rix, L., de Goeij, J.M., van Oevelen, D., Struck, U., Al-Horani, F.A., Wild, C., Naumann, M.S., 2017. Differential recycling of coral and algal dissolved organic matter via the sponge loop. Funct. Ecol. 31, 778–789. https://doi.org/10.1111/1365-2435.12758.

Rix, L., de Goeij, J.M., van Oevelen, D., Struck, U., Al-Horani, F.A., Wild, C., Naumann, M.S., 2018. Reef sponges facilitate the transfer of coral-derived organic

matter to their associated fauna via the sponge loop. Mar. Ecol. Prog. Ser. 589, 85–96. https://doi.org/10.3354/meps12443.
Rix, L., Ribes, M., Coma, R., Jahn, M.T., de Goeij, J.M., van Oevelen, D., Escrig, S., Meibom, A., Hentschel, U., 2020. Heterotrophy in the earliest gut: a single-cell view of heterotrophic carbon and nitrogen assimilation in sponge-microbe symbioses. ISME J. 14, 2554–2567. https://doi.org/10.1038/s41396-020-0706-3.
Rod'kina, S.A., 2005. Fatty acids and other lipids of marine sponges. Russ. J. Mar. Biol. 31, S49–S60. https://doi.org/10.1007/s11179-006-0015-3.
Romero, C.M., Engel, R.E., D'Andrilli, J., Chen, C., Zabinski, C., Miller, P.R., Wallander, R., 2017. Bulk optical characterization of dissolved organic matter from semiarid wheat-based cropping systems. Geoderma 306, 40–49. https://doi.org/10.1016/j.geoderma.2017.06.029.
Rybakova, E., Galkin, S., Gebruk, A., Sanamyan, N., Martynov, A., 2020. Vertical distribution of megafauna on the Bering Sea slope based on ROV survey. PeerJ 2020. https://doi.org/10.7717/peerj.8628.
Scheffers, S.R., Nieuwland, G., Bak, R.P.M., Van Duyl, F.C., 2004. Removal of bacteria and nutrient dynamics within the coral reef framework of Curaçao (Netherlands Antilles). Coral Reefs 23, 413–422. https://doi.org/10.1007/s00338-004-0400-3.
Senesi, N., 1990. Molecular and quantitative aspects of the chemistry of fulvic acid and its interactions with metal ions and organic chemicals. Anal. Chim. Acta 232, 77–106. https://doi.org/10.1016/S0003-2670(00)81226-X.
Simon, M., 2017. RV Sonne SO254 cruise report/ Fahrtbericht: SO254 - PoriBacNewZ: functional diversity of bacterial communities and the metabolome in the water column, sediment and in sponges in the Southwest Pacific around New Zealand. Oldenburg. https://doi.org/10.2312/cr_so254.
Spalding, M.D., Fox, H.E., Allen, G.R., Davidson, N., Ferdaña, Z.A., Finlayson, M., Halpern, B.S., Jorge, M.A., Lombana, A., Lourie, S.A., Martin, K.D., McManus, E., Molnar, J., Recchia, C.A., Robertson, J., 2007. Marine ecoregions of the world: a bioregionalization of coastal and shelf areas. Bioscience 57, 573–583. https://doi.org/10.1641/B570707.
Stedmon, C.A., Bro, R., 2008. Characterizing dissolved organic matter fluorescence with parallel factor analysis: a tutorial. Limnol. Oceanogr. Methods 6, 572–579. https://doi.org/10.4319/lom.2008.6.572.
Stedmon, C.A., Markager, S., 2005. Tracing the production and degradation of autochthonous fractions of dissolved organic matter by fluorescence analysis. Limnol. Oceanogr. 50, 1415–1426. https://doi.org/10.4319/lo.2005.50.5.1415.
Stedmon, C.A., Nelson, N.B., 2015. The optical properties of DOM in the ocean. In: Hansell, D.A., Carlson, C.A. (Eds.), Biogeochemistry of Marine Dissolved Organic Matter. Elsevier, Amsterdam, pp. 481–508. https://doi.org/10.1016/B978-0-12-405940-5.00010-8.
Stedmon, C.A., Markager, S., Bro, R., 2003. Tracing dissolved organic matter in aquatic environments using a new approach to fluorescence spectroscopy. Mar. Chem. 82, 239–254. https://doi.org/10.1016/S0304-4203(03)00072-0.
Stratmann, T., Simon-Lledó, E., Morganti, T.M., de Kluijver, A., Vedenin, A., Purser, A., 2022. Habitat types and megabenthos composition from three sponge-dominated high-Arctic seamounts. Sci. Rep. 12, 20610. https://doi.org/10.1038/s41598-022-25240-z.
Stratmann, T., Busch, K., de Kluijver, A., Kelly, M., Mills, S., Rossel, S., Schupp, P.J., 2024a. Nutrient fluxes, oxygen consumption and fatty acid composition from deep-water demo- and hexactinellid sponges from New Zealand. Deep-Sea Res. I Oceanogr. Res. Pap. 214, 104416. https://doi.org/10.1016/j.dsr.2024.104416.
Stratmann, T., Sahonero-Canavesi, D.X., van der Meer, M.T.J., 2024b. Combining ^{13}C, ^{15}N, and ^{2}H to measure feeding and metabolic activity in marine, shal-low-water sponges – a pilot study. bioRxiv preprint. https://doi.org/10.1101/2024.11.27.625585.
Thiel, V., Jenisch, A., Wörheide, G., Löwenberg, A., Reitner, J., Michaelis, W., 1999. Mid-chain branched alkanoic acids from "living fossil" demosponges: a link to ancient sedimentary lipids? Org. Geochem. 30, 1–14. https://doi.org/10.1016/S0146-6380(98)00200-9.
Thiel, V., Blumenberg, M., Hefter, J., Pape, T., Pomponi, S., Reed, J., Reitner, J., Wörheide, G., Michaelis, W., 2002a. A chemical view of the most ancient metazoa - biomarker chemotaxonomy of hexactinellid sponges. Naturwissenschaften 89, 60–66. https://doi.org/10.1007/s00114-001-0284-9.
Thiel, V., Blumenberg, M., Hefter, J., Pape, T., Pomponi, S., Reed, J., Reitner, J., Wörheide, G., Michaelis, W., 2002b. A chemical view of the most ancient metazoa - biomarker chemotaxonomy of hexactinellid sponges. Naturwissenschaften 89, 60–66. https://doi.org/10.1007/s00114-001-0284-9.
Trani, R., Corriero, G., de Pinto, M.C., Mercurio, M., Pazzani, C., Pierri, C., Scrascia, M., Longo, C., 2021. Filtering activity and nutrient release by the keratose sponge *Sarcotragus spinosulus* Schmidt, 1862 (Porifera, Demospongiae) at the laboratory scale. J. Mar. Sci. Eng. 9, 178. https://doi.org/10.3390/jmse9020178.
Vacelet, J., 1975. Étude en microscopie électronique de l'association entre bactéries et Spongiaires du genre Verongia (Dictyoceratida). J. Microsc. Biol. Cell. 23, 271–288.
Vacelet, J., Boury-Esnault, N., 1995. Carnivorous sponges. Nature 373, 333–335. https://doi.org/10.1038/373333a0.
Van Soest, R.W.M., Boury-Esnault, N., Vacelet, J., Dohrmann, M., Erpenbeck, D., De Voogd, N.J., Santodomingo, N., Vanhoorne, B., Kelly, M., Hooper, J.N.A., 2012. Global diversity of sponges (Porifera). PloS One 7, e35105. https://doi.org/10.1371/journal.pone.0035105.
Venables, W.N., Ripley, B.D., 2002. Modern Applied Statistics with S, 4th ed. Springer, New York City.
Verdugo, P., Alldredge, A.L., Azam, F., Kirchman, D.L., Passow, U., Santschi, P.H., 2004. The oceanic gel phase: a bridge in the DOM-POM continuum. In: Marine Chemistry. Elsevier B.V, pp. 67–85. https://doi.org/10.1016/j.marchem.2004.06.017.
Wagner, S., Jaffé, R., Cawley, K., Dittmar, T., Stubbins, A., 2015. Associations between the molecular and optical properties of dissolved organic matter in the Florida Everglades, a model coastal wetland system. Front. Chem. 3, 66. https://doi.org/10.3389/fchem.2015.00066.
Walker, S.A., Amon, R.M.W., Stedmon, C.A., 2013. Variations in high-latitude riverine fluorescent dissolved organic matter: a comparison of large Arctic rivers. J. Geophys. Res. Biogeosci. 118, 1689–1702. https://doi.org/10.1002/2013JG002320.
Webster, N.S., Taylor, M.W., 2012. Marine sponges and their microbial symbionts: love and other relationships. Environ. Microbiol. 14, 335–346. https://doi.org/10.1111/j.1462-2920.2011.02460.x.
Weisz, J.B., Lindquist, N., Martens, C.S., 2008. Do associated microbial abundances impact marine demosponge pumping rates and tissue densities? Oecologia 155, 367–376. https://doi.org/10.1007/s00442-007-0910-0.
Western, B., 1995. Concepts and suggestions for robust regression analysis. Am. J. Pol. Sci. 39, 786–817.
Wooster, M.K., McMurray, S.E., Pawlik, J.R., Morán, X.A.G., Berumen, M.L., 2019. Feeding and respiration by giant barrel sponges across a gradient of food abundance in the Red Sea. Limnol. Oceanogr. 64, 1790–1801. https://doi.org/10.1002/lno.11151.
Wurz, E., Beazley, L., MacDonald, B., Kenchington, E., Rapp, H.T., Osinga, R., 2021. The Hexactinellid deep-water sponge *Vazella pourtalesii* (Schmidt, 1870) (Rossellidae) copes with temporarily elevated concentrations of suspended natural sediment. Front. Mar. Sci. 8. https://doi.org/10.3389/fmars.2021.611539.
Wurz, E., Olsen, L.M.B., Busch, K., Ulvatn, T., Rapp, H.T., Osinga, R., Murk, A.J., 2024. Adverse effects of crushed seafloor massive sulphide deposits on the boreal deep-sea sponge *Geodia barretti* Bowerbank, 1858 and its associated fauna. Deep Sea Res. I Oceanogr Res. Pap. 208. https://doi.org/10.1016/j.dsr.2024.104311.
Yahel, G., Sharp, J.H., Marie, D., Häse, C., Genin, A., 2003. In situ feeding and element removal in the symbiont-bearing sponge *Theonella swinhoei*: bulk DOC is the major source for carbon. Limnol. Oceanogr. 48, 141–149. https://doi.org/10.4319/lo.2003.48.1.0141.
Yahel, G., Eerkes-Medrano, D.I., Leys, S.P., 2006. Size independent selective filtration of ultraplankton by hexactinellid glass sponges. Aquat. Microb. Ecol. 45, 181–194. https://doi.org/10.3354/ame045181.
Yamashita, Y., Tanoue, E., 2003. Chemical characterization of protein-like fluorophores in DOM in relation to aromatic amino acids. Mar. Chem. 82, 255–271. https://doi.org/10.1016/S0304-4203(03)00073-2.
Yamashita, Y., Cory, R.M., Nishioka, J., Kuma, K., Tanoue, E., Jaffé, R., 2010. Fluorescence characteristics of dissolved organic matter in the deep waters of the Okhotsk Sea and the northwestern North Pacific Ocean. Deep-Sea Res. II 57, 1478–1485. https://doi.org/10.1016/j.dsr2.2010.02.016.